Novel homodimeric and heterodimeric rat γ-hydroxybutyrate synthases that associate with the Golgi apparatus define a distinct subclass of aldo-keto reductase 7 family proteins

Vincent P. KELLY[1], Philip J. SHERRATT[2], Dorothy H. CROUCH and John D. HAYES[3]

Biomedical Research Centre, Ninewells Hospital and Medical School, University of Dundee, Dundee DD1 9SY, Scotland, U.K.

The aldo-keto reductase (AKR) 7 family is composed of the dimeric aflatoxin B_1 aldehyde reductase (AFAR) isoenzymes. In the rat, two AFAR subunits exist, designated rAFAR1 and rAFAR2. Herein, we report the molecular cloning of rAFAR2, showing that it shares 76% sequence identity with rAFAR1. By contrast with rAFAR1, which comprises 327 amino acids, rAFAR2 contains 367 amino acids. The 40 extra residues in rAFAR2 are located at the N-terminus of the polypeptide as an Arg-rich domain that may form an amphipathic α-helical structure. Protein purification and Western blotting have shown that the two AFAR subunits are found in rat liver extracts as both homodimers and as a heterodimer. Reductase activity in rat liver towards 2-carboxybenzaldehyde (CBA) was resolved by anion-exchange chromatography into three peaks containing rAFAR1-1, rAFAR1-2 and rAFAR2-2 dimers. These isoenzymes are functionally distinct; with NADPH as cofactor, rAFAR1-1 has a low K_m and high activity with CBA, whereas rAFAR2-2 exhibits a low K_m and high activity towards succinic semialdehyde. These data suggest that rAFAR1-1 is a detoxication enzyme, while rAFAR2-2 serves to synthesize the endogenous neuromodulator γ-hydroxybutyrate (GHB). Subcellular fractionation of liver extracts showed that rAFAR1-1 was recovered in the cytosol whereas rAFAR2-2 was associated with the Golgi apparatus. The distinct subcellular localization of the rAFAR1 and rAFAR2 subunits was confirmed by immunocytochemistry in H4IIE cells. Association of rAFAR2-2 with the Golgi apparatus presumably facilitates secretion of GHB, and the novel N-terminal domain may either determine the targeting of the enzyme to the Golgi or regulate the secretory process. A murine AKR protein of 367 residues has been identified in expressed sequence tag databases that shares 91% sequence identity with rAFAR2 and contains the Arg-rich extended N-terminus of 40 amino acids. Further bioinformatic evidence is presented that full-length human AKR7A2 is composed of 359 amino acids and also possesses an additional N-terminal domain. On the basis of these observations, we conclude that AKR7 proteins can be divided into two subfamilies, one of which is a Golgi-associated GHB synthase with a unique, previously unrecognized, N-terminal domain that is absent from other AKR proteins.

Key words: aflatoxin B_1 aldehyde reductase, 2-carboxybenzaldehyde, drug metabolism, succinic semialdehyde.

INTRODUCTION

Aldo-keto reductase (AKR) isoenzymes catalyse the NAD(P)(H)-dependent oxidation and/or reduction of alcohol- and carbonyl-containing compounds [1]. Substrates for these enzymes include endogenous compounds such as glucose, steroid hormones, prostaglandins and neurotransmitter aldehydes, as well as numerous xenobiotics [2–4]. The AKR superfamily has been divided on the basis of their primary structure into 12 separate families; proteins that share $> 40\%$ amino acid sequence identity are considered to be members of the same family. The AKR1 family is composed of mammalian aldehyde reductases, aldose reductases, hydroxysteroid dehydrogenases and steroid reductases. The AKR2–AKR5 families contain plant, yeast and bacterial enzymes. Members of the AKR6 family are regulatory β-subunits of voltage-gated K^+ channels that have been identified in mammals, invertebrates and plants. The AKR7 family comprises aflatoxin B_1 aldehyde reductase (AFAR) isoenzymes. Proteins included in AKR8 and AKR9 are pyridoxal reductases and aryl-alcohol dehydrogenases, respectively. Lastly, the remaining AKR10–AKR12 family members are prokaryotic oxidoreductases.

The crystal structures of human, pig and rodent AKR1 members have been solved [5–11]. Also, the crystal structures of yeast Gcy1p (AKR3A1) and bacterial 2,5-diketo-D-gluconic acid reductase (AKR5C) have been described [12,13]. These proteins are all soluble monomeric enzymes of approx. 320 amino acids that contain a parallel $(\alpha/\beta)_8$ barrel motif of the type found in triose phosphate isomerase.

Unlike AKR1 enzymes, the AKR6 family members are not soluble. Rather, they are membrane-associated polypeptides and adhere to the cytoplasmic surface of the pore-forming α-subunits of Shaker-related voltage-dependent Kv channels [14]. The AKR6 proteins regulate the gating activity of Kvα subunits [15],

Abbreviations used: AFAR, aflatoxin B_1 aldehyde reductase; AIAR, androgen-inducible aldehyde reductase; AKR, aldo-keto reductase; CBA, 2-carboxybenzaldehyde; CBA3–6, chromatography peaks 3–6 containing reductase activity towards CBA; CYP, cytochrome P450; DTT, dithiothreitol; ER, endoplasmic reticulum; EST, expressed sequence tag; GHB, γ-hydroxybutyrate; G58, Golgi 58 kDa protein; 4-NBA, 4-nitrobenzaldehyde; ORF, open reading frame; SSA, succinic semialdehyde; TRITC, tetramethylrhodamine isothiocyanate.

[1] Present address: Banyu Tsukuba Research Institute, Okubo 3, Tsukuba, Ibaraki 300-2611, Japan.

[2] Present address: Schering-Plough Research Institute, 2015 Galloping Hill Road, Kenilworth, NJ 07033, U.S.A.

[3] To whom correspondence should be addressed (e-mail john.hayes@cancer.org.uk).

The cDNA sequence for rat AFAR2 (also called AKR7A4) has been submitted to the GenBank Nucleotide Sequence Database under accession number AF503514. The cDNA sequences for mouse AFAR and human AKR7A2 have been submitted to the GenBank Third Party Annotation Database under accession numbers BK000393 and BK000395, respectively.

and are therefore most commonly called Kvβ subunits. These proteins contain the 'core' $(\alpha/\beta)_8$ barrel and can bind $NADP^+$ [16]. A feature of the AKR6 proteins that distinguishes them from AKR1 enzymes is that they exist as homotetramers. Furthermore, Kvβ subunits possess an additional N-terminal domain of between 19 and 50 amino acids, absent from AKR1 enzymes, that may be responsible for the rapid inactivation of Kv1 channels [17].

The founding member of the AKR7 family (i.e. AKR7A1) was the ethoxyquin-inducible rat liver AFAR [18,19], now called rAFAR1-1. This protein appears to play a cardinal role in cancer chemoprevention in the rat [20–22]. A further rat AKR7 polypeptide, designated rAFAR2, has been purified from liver cytosol [23,24]. Its cDNA has been cloned from rat prostate as an androgen-inducible aldehyde reductase (AIAR) [25]. Besides metabolizing aflatoxin B_1 [18,26], the rat AFAR enzymes exhibit high reductase activity towards 2-carboxybenzaldehyde (CBA) and succinic semialdehyde (SSA) [24,27]. Two additional members of this family, AKR7A2 and AKR7A3, have been identified in human tissues, and these also reduce aflatoxin B_1 dialdehyde, CBA and SSA [26–29].

Chromatography of CBA reductases in rat liver has led to the isolation of four ionically distinct peaks of enzyme activity containing reductase activity towards CBA, called CBA3–6, that cross-react with anti-human AKR7A2 serum [24]. The CBA3 peak comprised only the rAFAR1 subunit, whereas CBA4, CBA5 and CBA6 contained variable amounts of rAFAR1 and rAFAR2 subunits [24]. Gel filtration of these reductases on columns of Sephadex G-150 indicated that they have apparent native molecular masses of between 60 and 70 kDa, suggesting they are dimeric enzymes [23,24]. More recently, X-ray crystallography showed that rat AKR7A1 is composed of two identical subunits [30], confirming that CBA3 is indeed a homodimer of rAFAR1 subunits. At present, the relationship between CBA3 (i.e. rAFAR1-1) and CBA4, CBA5 and CBA6 is unclear.

In order to gain further insight into the structural relationships and physiological roles of the AKR7 enzymes, we have characterized the rat hepatic members of the family. Through use of molecular cloning and protein chemistry techniques, it has been found that the rAFAR2 subunit contains an additional 40-amino-acid N-terminal domain that is not present in rAFAR1, or indeed any other AKR protein. Purification of the CBA reductases from rat liver as rAFAR1 and rAFAR2 homodimers, along with the heterodimer, is described. In this paper these reductases are designated rAFAR1-1, rAFAR2-2 and rAFAR1-2. The two rAFAR2-containing enzymes were found to exhibit a low K_m value for SSA, suggesting that they act as γ-hydroxybutyrate (GHB) synthases *in vivo*. Subcellular fractionation and immunocytochemistry has indicated that the rAFAR2 subunit, but not rAFAR1, can associate with the Golgi apparatus, presumably facilitating the secretion of GHB.

MATERIALS AND METHODS

Chemicals, enzymes and molecular biology reagents

The chemicals used were of the highest quality available, and the sources have been described previously [24]. Econo-Pac cartidges of hydroxyapatite were obtained from Bio-Rad Laboratories (Hemel Hempsted, Herts., U.K.). Restriction enzymes were purchased from Gibco-BRL (Paisley, Scotland, U.K.). The λUnizap XL adult rat liver cDNA library, *Escherichia coli* XL1-Blue MRF′ cells and random prime labelling kit were from Stratagene (Cambridge, U.K.). *E. coli* BL21 pLysS was from Novagen (CN Biosciences, Beeston, Nottingham, U.K.).

Animals

Livers for enzyme purification were from 12 week-old male Fischer 344 rats. They were obtained as specimens that had been snap-frozen in liquid nitrogen (at the Cancer Research U.K. Biological Resource, Clare Hall, Potters Bar, Herts., U.K.) and transported to Dundee on dry ice, where they were stored at −70 °C. Livers for preparation of Golgi fractions were freshly isolated from 8 week-old female Sprague–Dawley rats that had been bred in the Medical School Animal Facility, University of Dundee, Scotland, U.K.

Cell culture

Rat H4IIE hepatoma cells, from the European Collection of Animal Cell Cultures, were grown in Earle's salts and glutaMAX-1™ (Eagle) supplemented with 1% (v/v) non-essential amino acids, 10% (v/v) foetal bovine serum and 50 units of penicillin/streptomycin.

Molecular cloning of rAFAR2

The cDNA for rAFAR2 was cloned from a λUnizap XL adult rat liver library, grown in *E. coli* XL1-Blue MRF′ cells, using a ^{32}P-radiolabelled random-primed probe from pLI18 that represents the coding region of human AKR7A2 [27].

Bacterial expression of rAFAR1-1 and rAFAR2-2

Heterologous expression of the rAFAR1 homodimer was performed in BL21 pLysS cells as described previously [31]. The rAFAR2-367 (full-length, codons 1–367) and rAFAR2-338 (N-terminal domain deleted, codons 30–367) dimers were synthesized in the *E. coli* BL21 pLysS strain. The rAFAR2-367 was amplified using 5′-CCGGAATTCATATGTTGCGTGCAGTGTC-3′ (forward) and 5′-CACCGCTCGAGCGACAGTCTATCTGAAGT-3′ (reverse; where the translation start site in the forward primer, and the stop site in the reverse primer, are shown underlined). rAFAR2-338 was amplified using 5′-CCGGAATTCATATGTCCCGGTCTCCGG-3′ (forward) in conjunction with the same reverse primer used above. The amplified products were digested with *Nde*I and *Xho*I before being ligated into similarly treated pET17b. Ligation products were transformed into *E. coli* NM522, and the fidelity of amplification was confirmed by sequencing. The expression construct was finally transformed into BL21 pLysS for bacterial synthesis of rAFAR2 polypeptides of known size.

Antibodies

Polyclonal EH630 antiserum against rAFAR1-1 was used [18], as this does not cross-react with the rAFAR2 polypeptide [24]. In addition, RW143 [27] was employed, as it cross-reacts with both the rAFAR1 and rAFAR2 subunits [24].

During the present study, antisera against heterologously expressed rAFAR2-2 (RW319, RW334 and RW335) were raised in female New Zealand white rabbits using standard methods. In order to increase the specificity of the antisera, those antibodies that cross-reacted with the rAFAR1 subunit were removed by passing the sera down a column of CNBr-activated Sepharose 4B to which rAFAR1-1 had been coupled.

The monoclonal antibody against cytochrome P450 (CYP) 1A1 was kindly provided by Dr Colin J. Henderson (Cancer Research U.K. Molecular Pharmacology Unit, Ninewells Hospital and Medical School, University of Dundee, Scotland,

U.K.). The monoclonal antibody against the Golgi 58 kDa protein (G58), FITC-conjugated goat anti-rabbit IgG, FITC-conjugated goat anti-mouse IgG and tetramethylrhodamine isothiocyanate (TRITC)-conjugated goat anti-rabbit IgG were purchased from Sigma–Aldrich Company (Poole, Dorset, U.K.). Affinity-purified, peroxidase-labelled goat anti-rabbit IgG antibodies were obtained from Bio-Rad Laboratories.

Biochemical analyses

Protein concentrations were measured by the Coomassie dye-binding assay [24]. Reductase activity was measured at 25 °C in 100 mM sodium phosphate buffer, pH 7.0. Activity towards various aldehydes (all at 1.0 mM) was examined using both NADPH and NADH as cofactors (at a concentration of 0.2 mM). The initial rate of reaction was monitored using a Cobas Fara centrifugal analyser (Hoffmann-La Roche, Basel, Switzerland) at 340 nm [27]. Kinetic parameters were determined by employing the Ultrafit curve-fitting software (Biosoft, Cambridge, U.K.) to fit the Michaelis–Menten equation using the Marquardt algorithm.

CYP activity was measured at 37 °C in PBS containing 4 μM 7-ethoxyresorufin by fluorescence spectroscopy with excitation at 530 nm and measurement of emission at 585 nm [32].

Discontinuous SDS/PAGE was performed as described previously [24], and proteins were stained with Coomassie Blue. For Western blotting, electrophoretic transfer of polypeptides from SDS/PAGE gels to nitrocellulose membranes was carried out with Bio-Rad equipment. Protein-binding sites on membranes were blocked by standard methods, and the blots were then incubated for 1 h at room temperature with antisera against AFAR subunits (at 1:2000 dilution). After washing, bound antibody was allowed to react for 1 h at room temperature with a horseradish peroxidase-conjugated secondary antibody (goat anti-rabbit IgG, at 1:3000 dilution). The antibody complexes were detected by enhanced chemiluminescence (ECL) and visualized following exposure to Blue-sensitive X-ray film (Genetic Research Instrumentation).

Isolation of AFAR isoenzymes from rat liver

Two methods were employed during this study to isolate these proteins from rat liver. Unless stated, all procedures were performed at 4 °C.

Purification method 1

The first purification scheme involved the use of Q-Sepharose, Matrex Orange A and Hi-Trap Blue [23,24]. The initial Q-Sepharose anion-exchange step resulted in the resolution of four enzyme-containing peaks with activity towards CBA, designated according to their order of elution as CBA3–CBA6. Thereafter, each of the four peaks was subjected in parallel to chromatography on Matrex Orange A and Hi-Trap™ Cibacron Blue F3G-A. The last chromatography step was performed at 20 °C.

Purification method 2

In the second purification scheme, a similar strategy to that described by Kelly et al. [24] was adopted, but a protease inhibitor was used during preparation of the cytosol, and an additional hydroxyapatite chromatography step was introduced immediately before chromatography on Hi-Trap™ Cibacron Blue F3G-A. Briefly, cytosol from 100 g of rat liver was prepared in 240 ml of ice-cold buffer A [10 mM Tris/HCl buffer, pH 8.2, 1 mM dithiothreitol (DTT) and 0.1 % (v/v) Triton X-100] containing five tablets of Complete™ protease inhibitor. Following dialysis against three changes, each of 5 l, of buffer A at 4 °C over 18 h, the material was centrifuged (10000 ***g***, 20 min, 4 °C) and applied to a 2.6 cm × 72.0 cm column of Q-Sepharose that was equilibrated with buffer A. This column was eluted at 32 ml/h and 4 °C with buffer A. After loading the sample on to the column, it was washed with 80 ml of buffer A before a linear salt gradient of 0–250 mM NaCl was applied in 1.2 l of buffer A. This was followed immediately by isocratic elution with 1 mM NaCl in the same buffer. The peaks corresponding to CBA3, CBA4 and CBA5 were pooled separately and dialysed against buffer B [10 mM sodium phosphate buffer, pH 8.0, containing 1 mM DTT and 0.1 % (v/v) Triton X-100]. The resulting CBA3, CBA4 and CBA5 pools were each applied to 1.6 cm × 1.4 cm columns of Matrex Orange A that were developed at 30 ml/h with a 0–1.5 M NaCl gradient in buffer B as described by Kelly et al. [24]. The fractions from the three Matrex Orange A columns containing reducing activity towards CBA were separately combined and dialysed against two changes, each of 5 l, of buffer C [10 mM potassium phosphate, pH 7.2, containing 1 mM DTT and 0.1 % (v/v) Triton X-100]. The dialysed samples were adjusted with buffer C to a volume of 40 ml before being applied to pre-packed Econo-Pac cartridges of hydroxyapatite that had also been equilibrated with buffer C. The CBA pools were eluted from the hydroxyapatite columns using a 10–250 mM potassium phosphate gradient formed in 400 ml of buffer pH 7.2 containing 1 mM DTT and 0.1 % (v/v) Triton X-100. At this stage, the CBA3 pool (i.e. rAFAR1-1) was homogeneous and was not subjected to further chromatography. The CBA4 and CBA5 pools were each combined, dialysed against buffer D [10 mM sodium phosphate, pH 7.0, 1 mM DTT and 0.1 % (v/v) Triton X-100], and applied separately to columns of Hi-Trap™ Cibacron Blue F3G-A. The column was developed with a linear 0–3.5 M NaCl gradient formed in buffer D between fractions 10 and 100; CBA4 eluted between fractions 40 and 45, whereas CBA5 eluted between fractions 34 and 40.

Preparation of Golgi-enriched hepatic subcellular fractions

This was performed using discontinuous sucrose gradients [33,34]. Portions (20 g) of rat livers were finely chopped in 35 ml of buffer E (100 mM potassium phosphate/5 mM $MgCl_2$, pH 6.7) containing 0.5 M sucrose and Complete™ EDTA-free protease inhibitor. The diced tissue was homogenized by gently pressing it through a 150 μm mesh sieve using the bottom of a glass conical flask as a pestle. Liver nuclei were removed by centrifugation at 1000 ***g*** for 10 min. The post-nuclear supernatant was adjusted to a volume of 26 ml with buffer E containing 0.5 M sucrose and Complete™ EDTA-free protease inhibitor, and 13 ml aliquots were overlaid on a discontinuous gradient that had been pre-prepared in a Sorvall 35 ml ultracentrifuge tube. This gradient comprised 7.5 ml of 1.3 M sucrose in buffer E, on top of which had been placed 13 ml of 0.86 M sucrose in buffer E. After the post-nuclear supernatant had been layered on top of the two sucrose phosphate-buffered solutions, the total volume was adjusted to 35 ml by adding dropwise about 1.5 ml of 0.25 M sucrose in buffer E. The gradient was established by centrifugation (100000 ***g***, 60 min) in a Sorvall swing-out bucket AH-629 rotor. Following centrifugation, the lipid layer was aspirated and discarded. Thereafter, 1 ml aliquots were withdrawn from the top of the gradient and placed in individual microfuge tubes. In each of these fractions across the gradient, reductase

activity towards CBA was measured and Western blotting was performed.

Cytosol was recovered in the layer containing 0.5 M sucrose. The Golgi apparatus partitioned into the layer formed between the buffer containing 0.5 M sucrose and 0.86 M sucrose. The smooth endoplasmic reticulum (ER) was found primarily in the 0.86 M sucrose-containing buffer, and the rough ER largely sedimented into the buffer containing 1.3 M sucrose.

Immunocytochemistry of rAFAR1 and rAFAR2 subunits

Rat hepatoma H4IIE cells were seeded on glass coverslips and grown in six-well culture plates. The cells were washed in PBS and fixed by treatment with 3% (w/v) paraformaldehyde in PBS for 10 min. Fixation and all following steps were carried out at room temperature. Cells were subsequently washed with PBS and permeabilized by incubating with 0.2% (v/v) Triton X-100 in PBS for 5 min. Non-specific sites were blocked using 0.5% (w/v) BSA in PBS (PBS/BSA). Slides were then incubated with polyclonal antisera raised against rAFAR1-1, rAFAR2-2 or a monoclonal antibody to G58 (Sigma), for 1 h at a final dilution of 1:100 in PBS/BSA. For co-localization studies, antibodies against rAFAR2-2 and G58 were incubated together. Cells were washed with PBS/BSA and incubated with the appropriate secondary antibody for 30 min diluted 1:100 in PBS/BSA. For single staining, FITC-conjugated goat anti-rabbit or goat anti-mouse IgG were employed. For co-localization studies, the rAFAR2-2 and G58 antibodies were detected using TRITC-conjugated goat anti-rabbit IgG and FITC-conjugated goat anti-mouse IgG respectively at a dilution of 1:100 in PBS/BSA. After thorough washing with PBS, the cells were mounted for fluorescence microscopy using Citifluor (Citifluor, London, U.K.) mounting media.

Cells were visualized by confocal microscopy using a Zeiss Axioplan 2 microscope, and images were captured using Zeiss LSM 510 software.

RESULTS

Molecular cloning of the cDNA for rAFAR2

The full-length clone for rAFAR2 was isolated by screening a λUnizap rat liver cDNA library with the human AKR7A2 probe. From approx. 3×10^5 plaques, nine positive clones were isolated. Restriction analysis and sequencing showed that three of these possessed an insert > 1250 bp. The longest of these, called pBS-C8, was found to contain a cDNA insert of 1274 bp (Figure 1). Sequencing of pBS-C8 revealed it comprised 6 bp of 5′-untranslated region, an open reading frame (ORF) of 1104 bp and 164 bp of 3′-untranslated region. The polyadenylation signal (AAUAAA) is positioned 16 nucleotides upstream of the poly(A) tail between nucleotides 1238 and 1243.

The clone for AIAR described previously by Nishi et al. [25] is 1271 bp in length, comprising 54 bp 5′-untranslated region, 1017 bp ORF and 200 bp 3′-untranslated region. Comparison between the clone for AIAR and pBS-C8 showed that the latter is 39 bp longer at the 5′-end than the AIAR clone. Significantly, pBS-C8 contains an upstream in-frame ATG initiation codon that is not present in the AIAR clone. Conversely, the 3′-end of the AIAR cDNA has 36 additional nucleotides [including a 29 bp poly(A) tail] that are missing from pBS-C8. A single coding change was noted between the rAFAR2 and AIAR clones. The rAFAR2 clone contains GAT (for Asp) at codon 295, whereas at this position the AIAR clone contains AGT (for Ser).

Although the nucleotide sequence comprising the ORF of pBS-C8 possesses approx. 75% identity with the same region of the cDNA for rAFAR1 [19], this high level of similarity does not exist over the first 140 nucleotides from the 5′-end of the clone.

The cDNAs for rAFAR2, a novel mouse AFAR protein and human AKR7A2 all encode polypeptides with a novel N-terminal domain

The polypeptide encoded by the rAFAR2 cDNA is predicted to comprise 367 amino acids (including the initiator Met) with a molecular mass of 40689 Da. The primary structure of the rAFAR2 protein can be aligned unambiguously with the variant 'core' AKR $(\alpha/\beta)_8$ barrel for the 7 family; the variant AKR7 core lacks loop A, possesses an extended loop B (or safety belt) and contains a shortened loop C [27,30]. It is however apparent that if the ATG at nucleotide 7 of pBS-C8 represents the translational start site, then rAFAR2 possesses an extended N-terminus of 40 amino acids that is not found in rAFAR1.

In order to determine whether the novel additional N-terminal domain is unique to rAFAR2, the possible existence of an orthologous mouse AKR7 protein was sought in cDNA databases. Computer-assisted searching of such databases revealed a RIKEN clone (GenBank accession number AK003915), a TIGR clone (THC781325) and five expressed sequence tag (EST) clones (AK002664, BE333646, BE652423, AI325523, BF147372) that encode a murine AFAR protein. As Figure 2 shows, this predicted mouse AFAR protein comprises 367 amino acids and shares 91% sequence identity with rAFAR2. Significantly, the cDNA possesses an ORF of 1104 bp that would be expected to translate into a polypeptide containing a domain equivalent to the extended N-terminus of rAFAR2.

Similar examination of the human EST database revealed that the mRNA for human AKR7A2 contains an ORF of 1080 bp encoding a polypeptide of 359 amino acids. It has been reported previously that AKR7A2 comprises 330 amino acids rather than 359 amino acids [27,28,35]. The 29 additional residues are to be found at the N-terminus, and arise because there exists an upstream in-frame ATG codon that was absent from previous AFAR cDNA clones [27,28,35]. The fact that four of the EST clones contain this first in-frame ATG codon (see BG386786, BG697637, BG386877 and BG828678) indicates that the additional N-terminal domain ought to be present in AKR7A2 protein in at least some human tissues. It is possible that variable processing of mRNA for AKR7A2 might influence whether it is translated into a polypeptide of 330 or 359 amino acids.

The predicted active centre of rAFAR2 is more closely related to those of mouse AFAR and human AKR7A2 than it is to that of rAFAR1

Comparison between the two rat AFAR polypeptides reveals that eight out of the 18 residues that are anticipated to form the substrate-binding site differ in the two proteins (Table 1). Specifically, Met^{84}, Asp^{87}, Asn^{115}, Trp^{117}, Asp^{118}, Ala^{150}, Trp^{264} and Thr^{267} in rAFAR2 are represented by Val^{44}, Asn^{47}, Ala^{75}, Met^{77}, Phe^{78}, Phe^{110}, Phe^{224} and Leu^{227} in rAFAR1. These substitutions suggest that the active centre of rAFAR2 can accommodate more hydrophilic substrates than rAFAR1. In mouse AFAR, only one difference exists amongst the 18 putative substrate-binding residues and rAFAR2, namely an Asp → Glu change at position 118. Similarly, comparison of the substrate-binding site in human AKR7A2 with that in rAFAR2 reveals a single $Ala^{150} \rightarrow Thr^{142}$ substitution. This suggests that rAFAR2, mAFAR and human AKR7A2 will all metabolize the same,

```
 -6                                                                GTCTTC

    Met Leu Arg Ala Val Ser Arg Ala Val Ser Arg Ala Ala Val Arg Cys Ala     17
  1 ATG TTG CGT GCA GTG TCC CGA GCG GTG AGC CGC GCT GCT GTA CGC TGC GCG
    Trp Arg Ser Gly Pro Ser Val Ala Arg Pro Leu Ala Met Ser Arg Ser Pro     34
 52 TGG CGC TCT GGG CCT TCG GTC GCG CGT CCT CTC GCC ATG TCC CGG TCT CCG
    Ala Pro Arg Ala Val Ser Gly Ala Pro Leu Arg Pro Gly Thr Val Leu Gly     51
103 GCA CCC CGC GCC GTC TCT GGC GCC CCT CTC CGG CCC GGT ACG GTG CTG GGC
    Thr Met Glu Met Gly Arg Arg Met Asp Ala Ser Ala Ser Ala Ala Thr Val     68
154 ACC ATG GAG ATG GGG CGC CGC ATG GAT GCG AGT GCT AGC GCT GCG ACC GTA
    Arg Ala Phe Leu Glu Arg Gly Leu Asn Glu Leu Asp Thr Ala Phe Met Tyr     85
205 CGC GCC TTC CTG GAG CGC GGC CTC AAC GAG CTG GAC ACG GCC TTC ATG TAT
    Cys Asp Gly Gln Ser Glu Ser Ile Leu Gly Ser Leu Gly Leu Gly Leu Gly    102
256 TGC GAC GGC CAG TCC GAA AGC ATC CTG GGC AGC CTG GGG CTC GGG CTG GGC
    Ser Gly Asp Cys Thr Val Lys Ile Ala Thr Lys Ala Asn Pro Trp Asp Gly    119
307 AGC GGC GAC TGC ACA GTG AAA ATT GCC ACC AAG GCC AAC CCT TGG GAC GGG
    Lys Ser Leu Lys Pro Asp Ser Val Arg Ser Gln Leu Glu Thr Ser Leu Lys    136
358 AAG TCG CTG AAG CCT GAC AGT GTC CGG TCC CAA TTA GAG ACG TCA TTG AAG
    Arg Leu Gln Cys Pro Arg Val Asp Leu Phe Tyr Leu His Ala Pro Asp His    153
409 CGG CTG CAG TGT CCC CGG GTG GAC CTC TTC TAC TTA CAC GCT CCT GAC CAC
    Gly Thr Pro Ile Val Glu Thr Leu Gln Ala Cys Gln Gln Leu His Gln Glu    170
460 GGC ACT CCT ATC GTG GAG ACC CTG CAG GCC TGC CAA CAG CTG CAT CAG GAG
    Gly Lys Phe Val Glu Leu Gly Leu Ser Asn Tyr Ala Ser Trp Glu Val Ala    187
511 GGC AAG TTT GTG GAG CTT GGC TTG TCC AAC TAT GCC TCC TGG GAG GTA GCC
    Glu Ile Tyr Thr Leu Cys Lys Ser Asn Gly Trp Ile Leu Pro Thr Val Tyr    204
562 GAG ATC TAT ACC CTC TGT AAA AGC AAC GGC TGG ATC CTG CCA ACT GTG TAC
    Gln Gly Met Tyr Asn Ala Thr Thr Arg Gln Val Glu Thr Glu Leu Leu Pro    221
613 CAG GGC ATG TAC AAC GCC ACC ACC CGG CAG GTG GAG ACT GAG CTC CTC CCC
    Cys Leu Arg Tyr Phe Gly Leu Arg Phe Tyr Ala Tyr Asn Pro Leu Ala Gly    238
664 TGC CTC AGA TAC TTC GGA CTG AGG TTC TAT GCC TAC AAC CCT TTG GCT GGA
    Gly Leu Leu Thr Gly Lys Tyr Arg Tyr Glu Asp Lys Asp Gly Lys Gln Pro    255
715 GGC CTG CTG ACT GGC AAA TAC AGA TAT GAA GAC AAG GAT GGG AAA CAG CCC
    Glu Gly Arg Phe Phe Gly Asn Ser Trp Ser Glu Thr Tyr Arg Asn Arg Phe    272
766 GAG GGC CGC TTC TTT GGG AAT AGC TGG TCT GAG ACC TAC AGG AAC CGC TTC
    Trp Lys Glu His His Phe Glu Ala Ile Ala Leu Val Glu Lys Ala Leu Lys    289
817 TGG AAG GAA CAC CAC TTT GAG GCC ATT GCC CTG GTA GAA AAG GCC CTG AAG
    Thr Thr Tyr Gly Thr Asp Ala Pro Ser Met Thr Ser Ala Ala Leu Arg Trp    306
868 ACC ACC TAT GGC ACC GAT GCC CCC AGC ATG ACC TCG GCT GCC CTG CGC TGG
    Met Tyr His His Ser Gln Leu Gln Gly Thr Arg Gly Asp Ala Val Ile Leu    323
919 ATG TAC CAT CAC TCA CAG CTC CAG GGC ACC CGA GGG GAC GCA GTC ATC TTG
    Gly Met Ser Ser Leu Glu Gln Leu Glu Gln Asn Leu Ala Ala Thr Glu Glu    340
970 GGC ATG TCC AGC CTG GAG CAG CTG GAG CAG AAC TTG GCG GCC ACT GAG GAA
    Gly Pro Leu Glu Pro Ala Val Val Glu Ala Phe Asn Gln Ala Trp Asn Val    357
1021 GGT CCC CTG GAG CCC GCT GTC GTG GAG GCC TTT AAC CAA GCC TGG AAC GTG
    Val Ala His Glu Cys Pro Asn Tyr Phe Arg Stop                          367
1072 GTC GCC CAC GAG TGT CCC AAC TAC TTC AGA TAG ACTGTCGTGACTCAAGACGCCAG

1128 GGCTTTTCTGCCAACTCTTAGAGTCACACCCTGGCCACTCCTTGCCCAGTGCTGACCTAGTGTGGTC
1195 TTTTCTGCTGGTCTCCATCCACTCCCTGCTCTTTTCCCGTCTGAATAAAGCAGGCGTCCGACCTAAA
1262 AAAAAAA
```

Figure 1 Molecular cloning of rAFAR2

The sequence of pBS-C8 is shown with the nucleotides numbered from the A of the first in-frame ATG codon. The polyadenylation signal AATAAA is underlined. The deduced amino acid sequence of the encoded protein is presented above the nucleic acid sequence, and numbered (see right-hand margin) from the presumed initiator Met. The amino acid sequence (M)YNATTRQVETELLPCL (residues 207–223) obtained from the CNBr digest of rAFAR2 [24] is underlined.

or closely similar, aldehydes. The residues that comprise the cofactor-binding site in the AKR7 members also appear to be highly conserved (Table 1).

Comparison of both primary structures and predicted active centres indicates that rAFAR2 is more closely related to mouse AFAR and human AKR7A2 than it is to rAFAR1. These data suggest that the AKR7 family can be subdivided into two distinct groups (Figure 3).

Confirmation that rAFAR2 contains a distinctive additional N-terminal domain

Characterization of pBS-C8 suggests that the rAFAR2 subunit is significantly larger than rAFAR1. This is surprising, given the fact that rAFAR2 migrates more quickly during SDS/PAGE than rAFAR1 [24]. Experiments were therefore undertaken to estimate the size of rAFAR2, and to establish which ATG codon

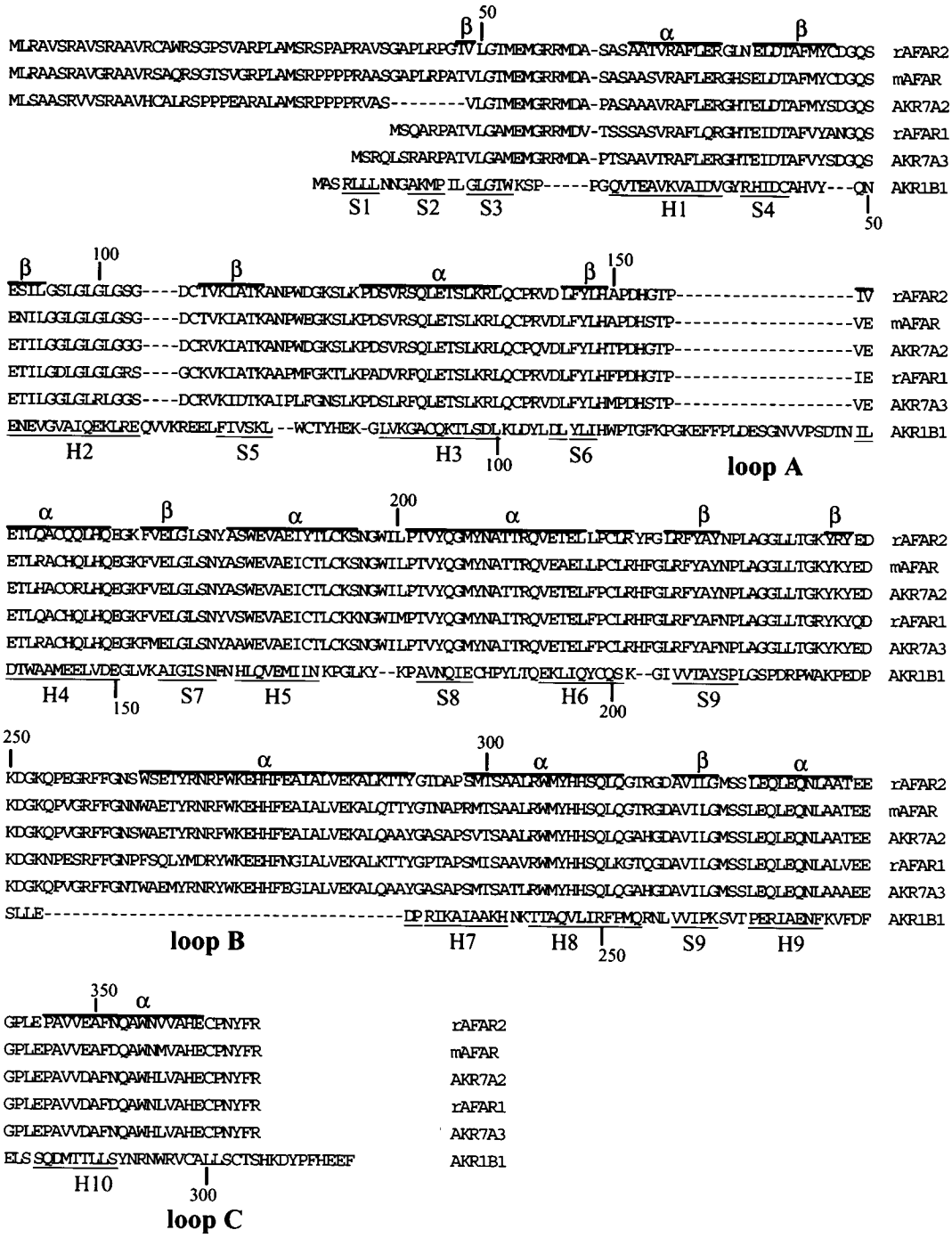

Figure 2 Comparison of rAFAR2 with other AKR

The primary structure of rAFAR2 (along with its predicted secondary structure) is aligned with that of mouse AFAR, full-length human AKR7A2, rAFAR1, human AKR7A3 and AKR1B1.

represents the translational start site. In Figure 1 the initiation codon is predicted to be located seven nucleotides from the 5′ end of the clone; accordingly, the first A is numbered +1. The next in-frame ATG codon, which resides at nucleotide +88, would yield a polypeptide of 338 amino acids (37611 Da), and this has been reported to be the translational start site of AIAR [25].

To get a more accurate estimate of the size of rAFAR2, the CBA5 enzyme was prepared by purification method 1, and analysed by desorption MS as well as automated N-terminal amino acid sequencing. Using a Finnigan Mat Lasermat instrument, rAFAR2 gave a molecular mass of 38189 Da; several components were identified in the CBA5 pool, indicating that it was not homogeneous. Edman degradation of CBA5 yielded the following four peptide sequences: AVSRAVS, AVSRAAV, SPAPRAV and AVSGAPL; these are encoded by nucleotides 10–30, 22–42, 97–117 and 112–132, respectively. Thus, both the

Table 1 Putative substrate- and cofactor-binding sites in rAFAR2 and the human and mouse AFAR subunits

Predictions of the residues in rat AFAR2, human AKR7A2 and AKR7A3, and mouse AFAR that contribute to substrate and cofactor binding are made from knowledge of the crystal structure of rAFAR1 (AKR7A1) [30]. The subunits are grouped together according to their sequence similarities shown in Figures 2 and 3. Thus, rAFAR2, mAFAR and AKR7A2 are grouped separately from rAFAR1 and AKR7A3. The numbering of the amino acids includes the initiator methionine.

Isoenzyme				
rAFAR2	mAFAR	AKR7A2	rAFAR1	AKR7A3
Substrate-binding residues				
Met^{53}	Met^{53}	Met^{45}	Met^{13}	Met^{17}
Arg^{57}	Arg^{57}	Arg^{49}	Arg^{17}	Arg^{21}
Asp^{80}	Asp^{80}	Asp^{72}	Asp^{40}	Asp^{44}
Met^{84}	Met^{84}	Met^{76}	Val^{44}	Val^{48}
Tyr^{85}	Tyr^{85}	Tyr^{77}	Tyr^{45}	Tyr^{49}
Asp^{87}	Asp^{87}	Asp^{79}	Asn^{47}	Asp^{51}
Lys^{113}	Lys^{113}	Lys^{105}	Lys^{73}	Lys^{77}
Asn^{115}	Asn^{115}	Asn^{107}	Ala^{75}	Ile^{79}
Trp^{117}	Trp^{117}	Trp^{109}	Met^{77}	Leu^{81}
Asp^{118}	Glu^{118}	Asp^{110}	Phe^{78}	Phe^{82}
His^{149}	His^{149}	His^{141}	His^{109}	His^{113}
Ala^{150}	Ala^{150}	Thr^{142}	Phe^{110}	Met^{114}
Asn^{262}	Asn^{262}	Asn^{254}	Asn^{222}	Asn^{226}
Trp^{264}	Trp^{264}	Trp^{256}	Phe^{224}	Trp^{228}
Thr^{267}	Thr^{267}	Thr^{259}	Leu^{227}	Met^{231}
Tyr^{268}	Tyr^{268}	Tyr^{260}	Tyr^{228}	Tyr^{232}
Arg^{271}	Arg^{271}	Arg^{263}	Arg^{231}	Arg^{235}
Arg^{367}	Arg^{367}	Arg^{359}	Arg^{327}	Arg^{331}
Cofactor-binding sites				
Arg^{58}	Arg^{58}	Arg^{50}	Arg^{18}	Arg^{22}
Asp^{80}	Asp^{80}	Asp^{72}	Asp^{40}	Asp^{44}
Ser^{179}	Ser^{179}	Ser^{171}	Ser^{139}	Ser^{143}
Asn^{180}	Asn^{180}	Asn^{172}	Asn^{140}	Asn^{144}
Gln^{205}	Gln^{205}	Gln^{197}	Gln^{165}	Gln^{169}
Tyr^{233}	Tyr^{233}	Tyr^{225}	Phe^{193}	Phe^{197}
Asn^{234}	Asn^{234}	Asn^{226}	Asn^{194}	Asn^{198}
Leu^{236}	Leu^{236}	Leu^{228}	Leu^{196}	Leu^{200}
Gly^{238}	Gly^{238}	Gly^{230}	Gly^{198}	Gly^{202}
Lys^{244}	Lys^{244}	Lys^{236}	Arg^{204}	Lys^{208}
Tyr^{245}	Tyr^{245}	Tyr^{237}	Tyr^{205}	Tyr^{209}
Pro^{255}	Pro^{255}	Pro^{247}	Pro^{215}	Pro^{219}
Gly^{257}	Gly^{257}	Gly^{249}	Ser^{217}	Gly^{221}
Arg^{258}	Arg^{258}	Arg^{250}	Arg^{218}	Arg^{222}
Gly^{324}	Gly^{324}	Gly^{316}	Gly^{284}	Gly^{288}
Met^{325}	Met^{325}	Met^{317}	Met^{285}	Met^{289}
Ser^{326}	Ser^{326}	Ser^{318}	Ser^{286}	Ser^{290}
Gln^{330}	Gln^{330}	Gln^{322}	Gln^{290}	Gln^{294}
Gln^{333}	Gln^{333}	Gln^{325}	Gln^{293}	Gln^{297}
Asn^{334}	Asn^{334}	Asn^{326}	Asn^{294}	Asn^{298}
Arg^{367}	Arg^{367}	Arg^{359}	Arg^{327}	Arg^{331}

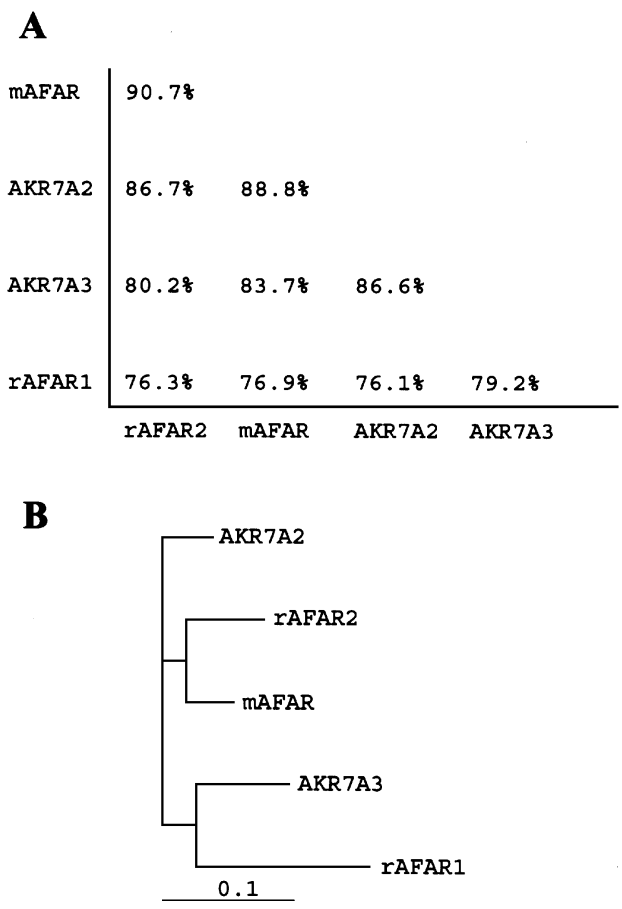

Figure 3 Pairwise identities of the AFAR proteins

The rAFAR2 and rAFAR1 sequences were compared with those of human AKR7A2 and AKR7A3 and that of mouse AFAR. (**A**) Pairwise identities that were calculated from the maximum region overlap using the ClustalW application (European Bioinformatics). (**B**) Dendrogram (generated from a pileup alignment; GCG Wisconsin) of the various AKR7 family members.

mass of rAFAR2 and the recovery of AVSRAVS and AVSRAAV from the native protein suggest that the first in-frame ATG represents the translational start site.

In order to confirm that rAFAR2 is indeed translated *in vivo* from the first in-frame ATG in the cDNA, bacterial expression constructs were made in pET17b that directed synthesis of the reductase from either the ATG at nucleotide +1 or from that at nucleotide +88. Once produced in *E. coli*, rAFAR2-367 (codons 1–367) and rAFAR2-338 (codons 30–367) were used as standards in Western blotting experiments of rat liver and the rat hepatocellular carcinoma H4IIE cell line. Probing immunoblots of rat liver cytosol and extracts from rat hepatoma cells with anti-AKR7A2 serum (RW143) gave two cross-reacting bands. The faster of these had an apparent molecular mass of 37 kDa, whereas the slower-migrating band had an apparent molecular mass of 38 kDa. These results are consistent with the previous observations of Kelly et al. [24]. Figure 4 shows the bacterially synthesized rAFAR2-367 co-migrated with the immunoreactive rat polypeptide of greatest mobility (apparent molecular mass of 37 kDa). By contrast, rAFAR2-338 was found to have a faster anodal mobility than any of the immunoreactive proteins in rat liver or H4IIE cells. Furthermore, heterologously expressed rAFAR1 was shown to co-migrate with the slower, more cathodal, of the two immunoreactive bands.

Collectively, these results suggest that *in vivo* the rAFAR2 subunit consists of a polypeptide of 367 amino acids that includes an N-terminal domain of 40 amino acid residues that is not represented in rAFAR1.

Subunit composition of CBA reductases from rat liver

The quaternary structure of the different forms of AFAR in the rat is unclear. It has been shown that four CBA reductase peaks containing either rAFAR1 and/or rAFAR2 subunits can be resolved from rat liver cytosol by anion-exchange chromatography [24]. The amino acid sequencing results presented above provided evidence that the N-terminus of rAFAR2 can be processively cleaved. The purification scheme was therefore

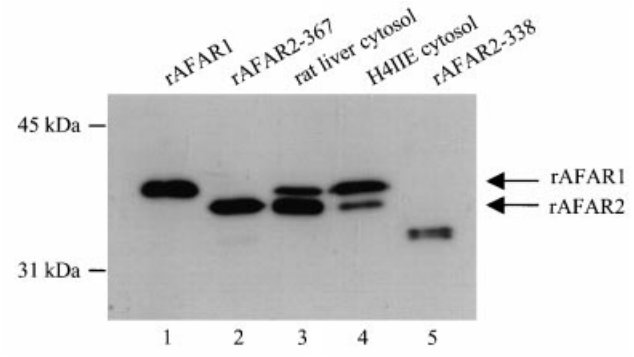

Figure 4 Comparative electrophoretic mobilities of recombinant rAFAR2 proteins with that of the native protein

Recombinant rAFAR1, rAFAR2-367 and rAFAR2-338 polypeptides were synthesized in *E. coli* BL21 pLysS as described in the Materials and methods section. Portions of bacterial samples (10 μg of protein) containing the AFAR proteins along with portions of rat liver cytosol and extracts of rat H4IIE hepatocytes (10 μg of protein) were subjected, in parallel, to SDS/PAGE in a Bio-Rad Protean II xi Cell apparatus. The samples were loaded as follows: lane 1, recombinant rAFAR1 protein; lane 2, recombinant rAFAR2 containing 367 amino acids; lane 3, rat liver cytosol; lane 4, extract from rat liver H4IIE cells; lane 5, recombinant rAFAR2 containing 338 amino acids. Once resolved, proteins were transferred to Immobilon-P membranes and probed with RW143 antibodies raised against human AKR7A2. The cross-reacting bands were located using a peroxidase-labelled goat anti-rabbit IgG, and visualized by ECL. The position of molecular-mass markers (kDa) is shown on the left.

modified to minimize proteolysis, and to improve resolution of the different forms of AFAR. To this end, Complete™ protease inhibitor was added to buffers employed to prepare hepatic cytosol for anion-exchange chromatography on Q-Sepharose, and a hydroxyapatite step was included in the purification scheme.

Figure 5 shows that in the presence of protease inhibitor, the CBA reductase activity in rat liver is eluted from Q-Sepharose as three peaks, CBA3, CBA4 and CBA5. The failure to recover CBA6 under these experimental conditions suggests it represents a proteolytic degradation product. Following further chromatography on columns of Matrex Orange A, hydroxyapatite and Hi-Trap™ Cibacron Blue F3G-A, CBA3, CBA4 and CBA5 were purified 140-, 240- and 130-fold, respectively. Electrophoretic examination of the preparations indicated that they were homogeneous; CBA3 comprised subunits of apparently 38 kDa, CBA4 comprised two distinct subunits of 37 kDa and 38 kDa, and CBA5 comprised subunits of apparently 37 kDa (Figure 6A).

The CBA3, CBA4 and CBA5 proteins were probed with antibodies raised against recombinant rAFAR1 and rAFAR2 subunits. In immunoblotting experiments, CBA3 and CBA4 cross-reacted with anti-rAFAR1 serum, whereas CBA4 and CBA5 cross-reacted with anti-rAFAR2 serum (Figures 6B and 6C). These data, together with previous gel-filtration chromatography data [23,24], indicate that CBA3, CBA4 and CBA5 represent rAFAR1-1, rAFAR1-2 and rAFAR2-2, respectively.

The rAFAR isoenzymes are catalytically distinct

Although the catalytic activity of rAFAR1-1 has been thoroughly studied, little is known about the function of either rAFAR1-2 or rAFAR2-2. The specific activities of the three isoenzymes towards a number of aldehydes have therefore been determined. Table 2 shows that amongst the three reductases, the specific activity (under standard assay conditions) towards SSA with NADH as cofactor was as follows: rAFAR2-2 > rAFAR1-2 > rAFAR1-1. With SSA and NADPH as cofactor, rAFAR2-2 again had the highest specific activity of the three reductases, but rAFAR1-2 appeared to be less active than rAFAR1-1. By contrast, with CBA as substrate and NADH as cofactor, the relative activity was rAFAR1-1 > rAFAR1-2 > rAFAR2-2 (Table 2). When 4-nitrobenzaldehyde (4-NBA) was employed as substrate, the relative activities, with either cofactor, were rAFAR1-1 > rAFAR1-2 > rAFAR2-2. The converse was observed using benzaldehyde and NADPH as cofactor.

The kinetic properties of the two rAFAR homodimers provided a further insight into their functional relationship. Table 3

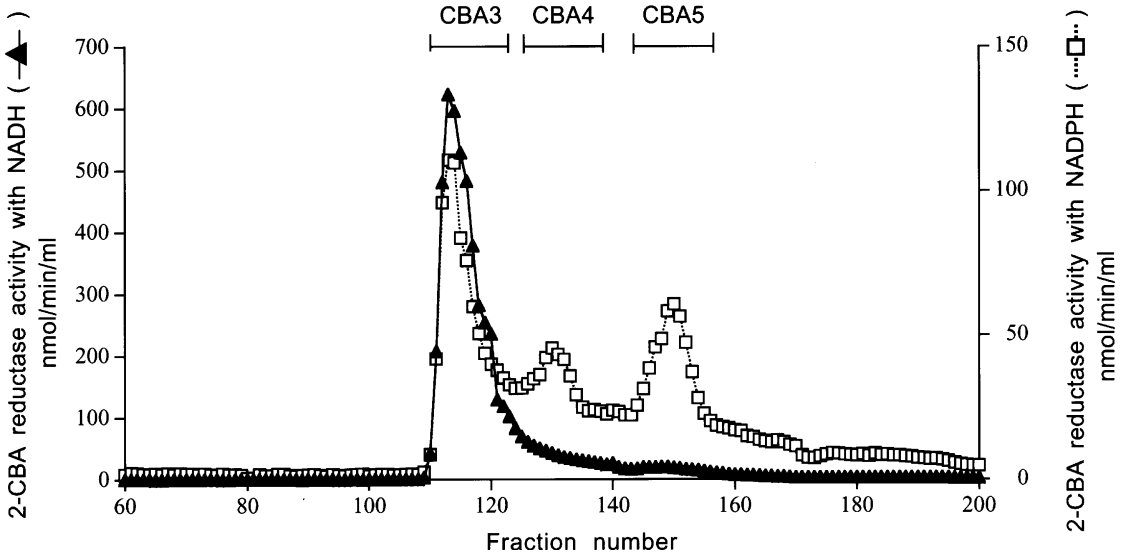

Figure 5 Resolution of CBA reductase activity in rat liver

Rat liver cytosol was prepared in buffer A containing Complete™ protease inhibitor, as described in the Materials and methods section. After dialysis against buffer A, the hepatic cytosol was applied (32 ml/h) to a 2.6 cm × 72.0 cm column of Q-Sepharose. Fractions (8 ml) were collected and a linear 0–250 mM NaCl gradient was applied between fractions 35 and 175. The activity towards CBA was measured with either NADH (▲) or NADPH (□).

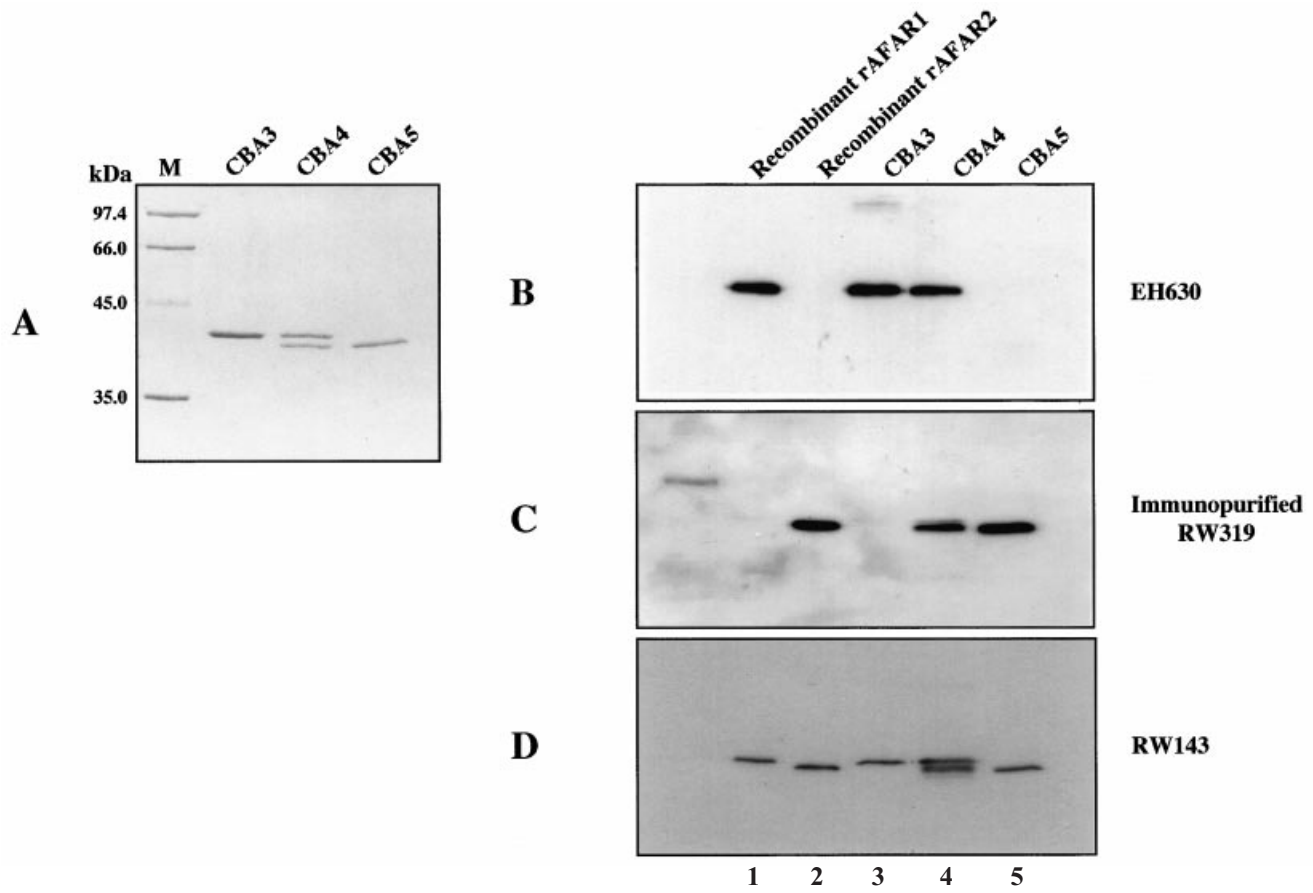

Figure 6 Electrophoretic and immunochemical analysis of CBA reductases

The AKR isoenzymes with activity towards CBA were purified as described in the text. (**A**) SDS/PAGE of CBA3, CBA4 and CBA5 stained with Coomassie Brilliant Blue R250. Molecular-mass markers (M) and their sizes (kDa) are shown. (**B**–**D**) Immunoblots of bacterially expressed rAFAR1-1 and rAFAR2-2, along with CBA3, CBA4 and CBA5 probed with antiserum EH630 (specific for rAFAR1), affinity-purified RW319 (specific for rAFAR2) and RW143 (recognizes both rAFAR1 and rAFAR2 subunits). Note that in the left-hand margin of panel C, the 45 kDa standard has cross-reacted with RW319 antiserum. This margin track has not been included in the AFAR-containing lanes numbered 1–5.

Table 2 Specific activity of AFAR isoenzymes towards aldehydes

The assays were performed at 25 °C with 1.0 mM SSA, CBA, 4-NBA or benzaldehyde and 0.2 mM NADPH or NADH.

			Specific activity (nmol/min per mg of protein)		
		Enzyme ...	rAFAR1-1	rAFAR1-2	rAFAR2-2
Substrate	Cofactor	Q-Sepharose pool ...	CBA3	CBA4	CBA5
SSA	NADPH		680 ± 10	570 ± 10	930 ± 10
	NADH		50 ± 2	640 ± 2	1710 ± 40
CBA	NADPH		1530 ± 10	920 ± 10	1090 ± 10
	NADH		4360 ± 60	2810 ± 50	1220 ± 30
4-NBA	NADPH		380 ± 10	160 ± 10	75 ± 5
	NADH		65 ± 5	14 ± 2	4 ± 0.4
Benzaldehyde	NADPH		80 ± 5	280 ± 10	730 ± 10

Table 3 Kinetic properties of rat AFAR isoenzymes

The catalytic activities of AFAR isoenzymes towards succinic semialdehyde and CBA were determined at 25 °C using 0.2 mM NADPH as cofactor. The k_{cat} value was calculated using molecular masses for rAFAR1-1, rAFAR1-2 and rAFAR2-2 of 73.4 kDa, 77.4 kDa and 81.4 kDa, respectively.

Substrate	Enzyme	K_m (μM)	k_{cat} (min^{-1})	k_{cat}/K_m ($min^{-1} \cdot M^{-1}$)
SSA	rAFAR1-1	163 ± 25	93.6 ± 1.8	5.72×10^5
	rAFAR1-2	8.8 ± 0.7	33.0 ± 2.2	3.73×10^6
	rAFAR2-2	6.4 ± 0.6	76.6 ± 1.0	1.19×10^7
CBA	rAFAR1-1	0.7 ± 0.2	164.8 ± 15.2	2.29×10^8
	rAFAR1-2	0.5 ± 0.1	42.8 ± 3	9.95×10^7
	rAFAR2-2	9.7 ± 0.2	82.3 ± 0.9	8.50×10^6
NADPH (with CBA)	rAFAR1-1	1.66 ± 0.19	120.2 ± 10.5	7.26×10^7
	rAFAR1-2	1.76 ± 0.21	92.8 ± 3.8	5.27×10^7
	rAFAR2-2	1.46 ± 0.12	85.5 ± 8.2	5.86×10^7

shows that rAFAR2-2 has a substantially lower K_m for SSA than rAFAR1-1. Conversely, rAFAR1-1 has a lower K_m for CBA than rAFAR2-2. Both rAFAR isoenzymes were found to have similar K_m values for NADPH. The K_m of rAFAR2-2 for SSA is sufficiently low for the aldehyde to represent an important substrate *in vivo*. These data therefore suggest that a physiological function of rAFAR2-2 is to serve as a GHB synthase, whereas rAFAR1-1 probably acts to detoxify CBA and other xenobiotics.

Table 4 Sensitivity of AFAR isoenzymes to model inhibitors

Enzyme activity was measured at 25 °C using 1.0 mM SSA and 0.2 mM NADPH. In the absence of an inhibitor, the activities of rAFAR1-1, rAFAR1-2 and rAFAR2-2 towards SSA were 680, 570 and 930 nmol/min per mg, respectively.

Inhibitor	Concentration (mM)	Enzyme ...	SSA reductase activity remaining (%)		
			rAFAR1-1	rAFAR1-2	rAFAR2-2
None	–		100	100	100
Barbital	1.0		98	98	100
Pentobarbital	1.0		96	98	100
Phenobarbital	1.0		81	97	100
Oxalate	1.0		85	78	68
Valproate	1.0		67	90	96
Diphenylhydantoin	0.2		100	99	98
Indomethacin	0.1		26	39	41
Quercitin	0.01		38	64	67
Citrate	1.0		33	41	33
GHB	1.0		96	95	93

The inhibition profile of rAFAR isoenzymes resembles that of the SSA reductase in rat

It has been reported that the specific SSA reductase(s) in rat brain can be distinguished from the non-specific SSA reductases in that it is insensitive to inhibition by barbiturates, diphenylhydantoin or valproate [36,37]. Purified rAFAR1-1, rAFAR1-2 and rAFAR2-2 were therefore challenged with these xenobiotics. Under standard assay conditions, barbital, pentobarbital or diphenylhydantoin had little effect on the SSA reductase activity of the rat AFAR isoenzymes. However, phenobarbital affected an approx. 20% inhibition of rAFAR1-1, but not rAFAR1-2 or rAFAR2-2 (Table 4). Treatment with valproate resulted in approx. 30% inhibition of rAFAR1-1, but it inhibited neither rAFAR1-2 nor rAFAR2-2 (Table 4). Based on the resistance of rAFAR1-2 and rAFAR2-2 to inhibition by phenobarbital and valproate, these two enzymes may have contributed to the specific SSA reductase activity in rat brain described by Tabakoff and von Wartburg [36] or Rumigny et al. [37].

The rAFAR2 subunit is recovered from rat liver in membrane-enriched subcellular fractions

Since rAFAR2 possesses an N-terminal extension and secondary-structure features that are reminiscent of the membrane-associated AKR6 family proteins, it was decided to examine the subcellular distribution of rAFAR2-2. For this purpose, rat liver was resolved into cytosolic, Golgi apparatus, smooth ER and rough ER fractions using discontinuous sucrose gradient centrifugation.

Portions of fractions across the gradient were assayed for AKR activity. When a low concentration of SSA (i.e. 25 μM) and 0.2 mM NADPH was employed in the enzyme assay, most

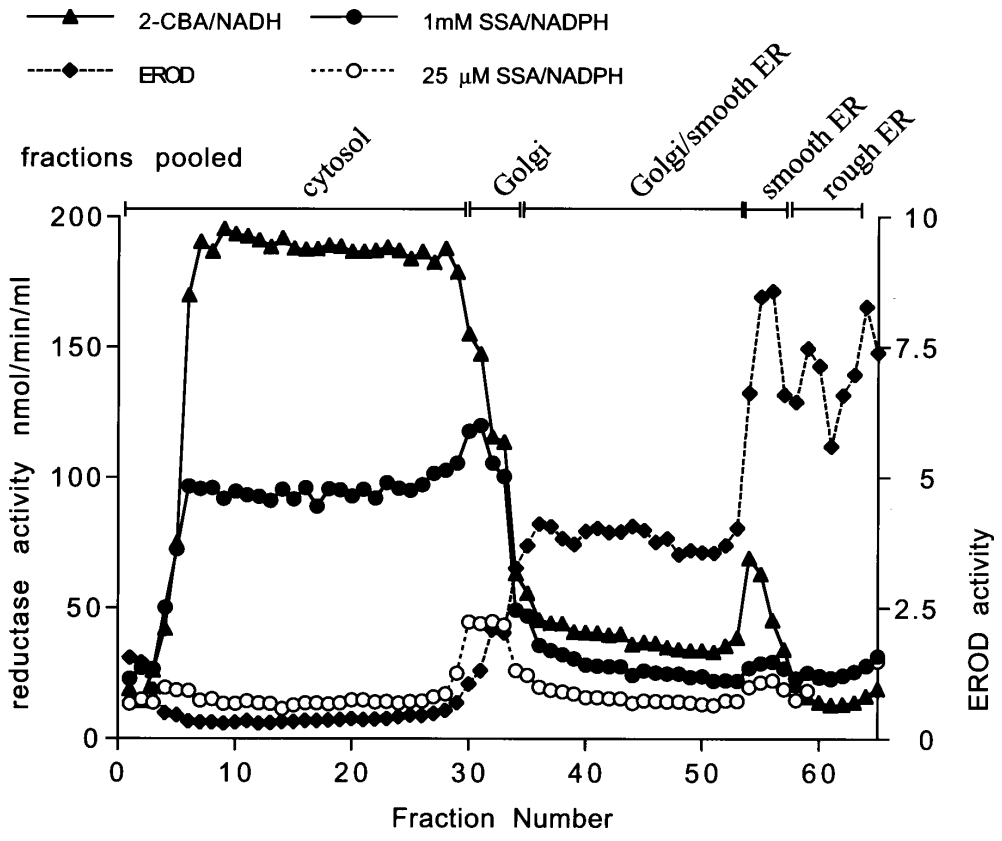

Figure 7 Differential distribution of AKR activities in hepatic subcellular fractions

Rat hepatic cytosol, Golgi, smooth ER and rough ER were prepared by discontinuous sucrose gradient centrifugation, and 1 ml aliquots were withdrawn sequentially from the top of the gradient. The fractions obtained were as follows: cytosol, fractions 1–29; Golgi apparatus, fractions 30–34; Golgi/smooth ER ('layer B'), fractions 35–53; smooth ER, fractions 54–57; rough ER, fractions 58–63. The AKR activity in these fractions was determined using 1 mM SSA and 200 μM NADPH (●), 25 μM SSA and 200 μM NADPH (○), 1 mM CBA and 200 μM NADH (▲), or 4 μM 7-ethoxyresorufin (EROD) to monitor CYP (◆). EROD activity is shown in arbitrary units calculated as the increase in fluorescence emission at 585 nm.

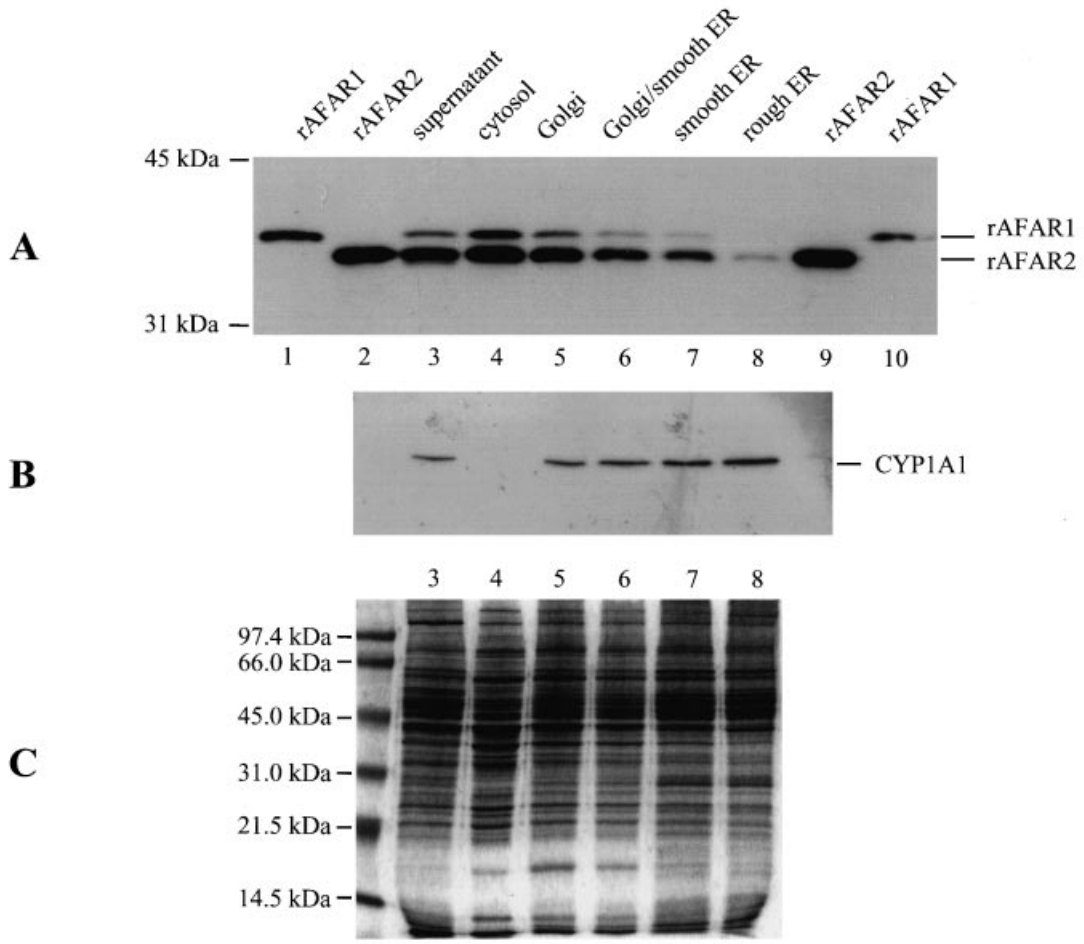

Figure 8 Subcellular distribution of AFAR subunits and comparison with CYP1A1

Rat liver subcellular fractions were prepared by ultracentrifugation as shown in Figure 7. Samples were applied to SDS/PAGE gels for Western blotting as follows: lanes 1 and 10, bacterially-expressed rAFAR1-1; lanes 2 and 9, bacterially-expressed rAFAR2-2; lane 3, post-nuclear supernatant; lane 4, cytosol; lane 5, Golgi; lane 6, Golgi/smooth ER; lane 7, smooth ER; lane 8, rough ER. (**A**) Blot probed with RW143, which cross-reacts with rAFAR1 and rAFAR2. (**B**) Blot probed with monoclonal antibodies against CYP1A1. (**C**) SDS/PAGE of the post-nuclear supernatant, cytosolic, Golgi, Golgi/smooth ER, smooth ER and rough ER liver fractions stained with Coomassie Brilliant Blue R250, to demonstrate approximately equivalent loading of the polyacrylamide gel.

of the reductase activity was found to reside in the Golgi-containing fractions, though a small amount was also detected in ER-containing fractions (Figure 7). However, when a higher concentration of SSA (i.e. 1 mM) along with 0.2 mM NADPH was used in the assay, the majority of the reductase activity was found in the cytosol-containing fractions. From a knowledge of the K_m values of the reductases for SSA, it was considered likely that rAFAR2-2 would account for the majority of the enzymic activity when 25 μM SSA was employed in the assay. Therefore, these results suggest that rAFAR2-2, and not rAFAR1-1, can associate with the Golgi apparatus and ER.

Fractions across the gradient were also assayed for their ability to reduce CBA. With NADH as cofactor, most of the CBA reductase activity was found in the cytosol, a finding that supports the notion that rAFAR1-1 is primarily cytoplasmic.

As an internal control in these experiments, cytochrome P450 activity was also measured, and as expected it was found to be almost entirely associated with the ER-containing fractions.

The sucrose gradient was analysed by Western blotting to determine which fractions contained the rAFAR2 and rAFAR1 subunits; CYP1A1 was used as an internal control. Using the RW143 antibody, large amounts of rAFAR2 were detected in the cytosol and Golgi fractions, with lesser amounts being observed in fractions corresponding to the smooth ER, and trace amounts in the rough ER (Figure 8). This antibody also revealed that rAFAR1 was primarily recovered in the cytosolic fraction, though it was also clearly detected in the Golgi-containing fraction. However, rAFAR1 was essentially absent from both smooth ER and rough ER. Probing these blots with anti-CYP1A1 serum showed the cytochrome was absent from cytosol, but was present in Golgi, smooth ER and rough ER.

Immunofluorescence microscopy of AFAR isoenzymes

Immunostaining rat H4IIE monolayers with either RW143 or RW319 yielded an intense fluorescent signal on intracellular structures with the appearance and localization of Golgi cisternae. The interpretation that these antibodies recognize rAFAR2 subunits that are associated with the Golgi apparatus was confirmed by double-labelling experiments using both anti-rAFAR2 serum and antibodies against G58. As Figure 9 shows,

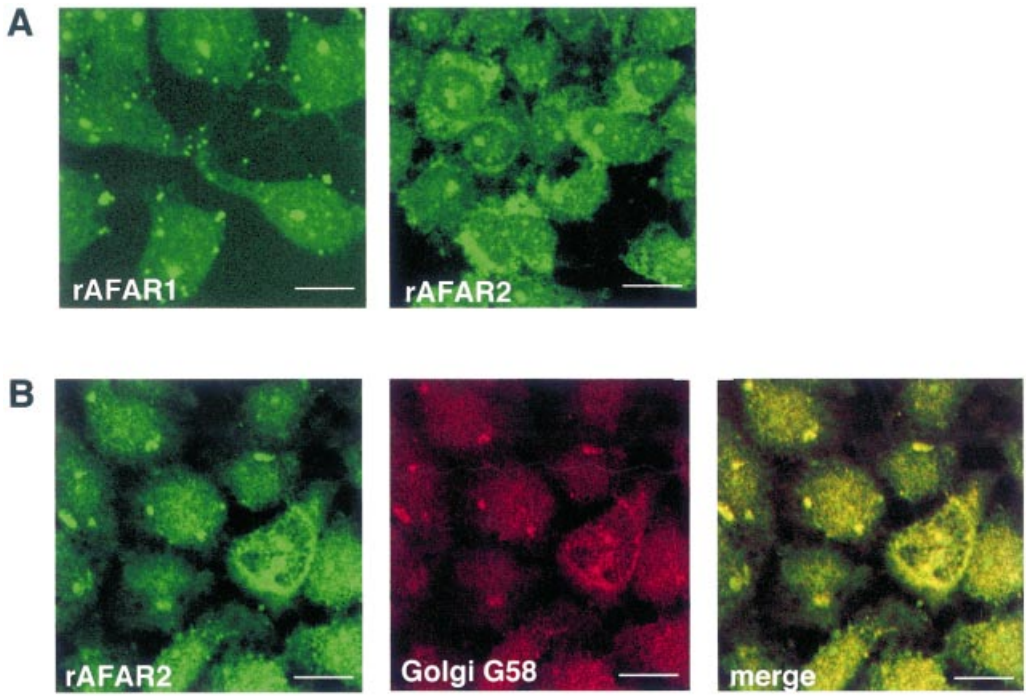

Figure 9 Localization of rAFAR1 and rAFAR2 subunits in rat H4IIE hepatoma cells

(**A**) The rAFAR1 and rAFAR2, detected using specific rabbit antibodies and FITC-conjugated anti-rabbit IgG, were visualized by confocal microscopy using a Zeiss Axioplan 2 microscope. (**B**) Co-localization of AFAR2 and the Golgi protein G58 was shown by co-staining with rabbit and mouse primary antibodies respectively. Following incubation with the appropriate fluorochrome-conjugated secondary antibody, co-localization was visualized by confocal microscopy. Scale bars, 10 μm.

merging the signal obtained from both antibodies demonstrated that they co-localized.

By contrast with results for rAFAR2, immunofluorescence microscopy of H4IIE cells with the EH630 antibody yielded a uniform cytoplasmic staining, occupying the whole cell volume, with a relatively negative nucleus, indicative of a cytoplasmic soluble protein.

DISCUSSION

Western blotting originally provided evidence for the existence of a second AFAR polypeptide in rat liver [23,24]. These earlier experiments employed antibodies against human AKR7A2 to identify in rat liver an enzyme that is chromatographically and electrophoretically distinct from rAFAR1-1. The present study describes molecular cloning of rAFAR2-2, and characterization of its biochemical properties as well as its subcellular localization.

Structure of the N-terminus of rAFAR2

The most unexpected feature of rAFAR2 is that it contains 40 more amino acids at its N-terminus than does rAFAR1. This extended N-terminus primarily comprises neutral and hydrophobic amino acids, but it also contains eight Arg residues at positions 3, 7, 11, 15, 19, 26, 32 and 37. Not only are the basic Arg residues evenly distributed within the domain, but it is also apparent that hydrophobic Ala, Val, Cys and Trp residues are similarly located regularly throughout this region. If it were possible for this N-terminal domain to adopt a classical α-helical structure, with 3.4 residues per turn and a pitch of 5.4 Å, then the arginines would be placed along one face of the α-helix with each residue interspersed with a hydrophobic amino acid. This putative amphipathic helix might allow ionic interactions with another polypeptide. Alternatively, this domain could allow a coiled-coil structure to form between two rAFAR2 subunits, or between rAFAR2 and another protein.

Amino acid sequencing showed that the N-terminus of rAFAR2 is susceptible to proteolysis, a finding that implies this region is exposed during protein purification. At least two possible functions might be ascribed to the N-terminus of rAFAR2. Firstly, it could be responsible for targeting the subunit to the Golgi apparatus. Secondly, by analogy with the additional N-terminal domain of Kvβ subunits, it could serve a role in regulating conductance channels. Such an activity might be coupled with the Ca^{2+}-dependent secretion of GHB [38].

The N-terminal domain of rAFAR2 defines a subclass within the AKR7 family that is represented in murine and human AFAR subunits

The existence of the additional domain within rAFAR2 raised the question of whether it is represented in other species. Examination of the RIKEN and TIGR databases revealed the existence of a mouse AFAR polypeptide that also contains a similar extended N-terminus. At the amino acid level, this additional N-terminal domain in murine AFAR shares 78% sequence identity with the same region in the rat reductase. The eight Arg residues at positions 3, 7, 11, 15, 19, 26, 32 and 37 in rAFAR2 are all conserved in the mAFAR subunit (Figure 2).

Examination of the human EST database revealed that the mRNA for AKR7A2 encodes a polypeptide that also contains the novel additional N-terminal domain. At the amino acid level this region in AKR7A2 shares 68% identity with the same region in rAFAR2 and also 68% identity with the N-terminus of

mAFAR (Figure 2). Interestingly, AKR7A2 contains six of the eight Arg residues (at positions 7, 11, 19, 26, 32 and 37) in this domain that are present in the rodent proteins. The Arg at position 3 in rAFAR2 is replaced by Ser in AKR7A2, and the Arg at position 15 in rAFAR2 is replaced by His in AKR7A2. Previous purification of AKR7A2 from human liver failed to identify the additional N-terminal domain [27]. It is difficult to conclude that *in vitro* proteolysis accounted for this failure, because the N-terminal amino acid was immediately adjacent to a Met residue (i.e. Met^{30}). It is likely that a cytoplasmic form of AKR7A2 can be synthesized using the second in-frame ATG, and that this may be regulated by alternative splicing pathways. Whether there are distinct Golgi and cytoplasmic forms of AKR7A2 is a question that should be addressed in future studies.

Comparison between the three N-termini reveals that 23 of the 40 residues are present in the rat, mouse and human proteins. A consensus sequence for this novel domain can therefore be proposed that is rich in Arg and Ala residues: MLXAXS-RXVXRAAVXXAXRSXXXXXRXLAMSRXPXPRXXS. The remaining 17 residues, where variation has arisen, include a number of conservative substitutions, for example, four Ala → Val, one Ala → Gly, one Cys → Ser and one Arg → His, at positions 5, 8, 15, 16, 25, 38 and 39. It therefore appears that the putative amphipathic helical structure of the domain may also be represented in mouse AFAR and human AKR7A2.

Dimeric structure of AKR7 enzymes

Molecular cloning experiments have shown rAFAR1 contains 327 amino acids with a molecular mass of 36742 Da [19], and rAFAR2 contains 367 amino acids with a molecular mass of 40689 Da (Figure 1). Estimation of the native molecular masses of rAFAR1- and rAFAR2-containing CBA reductases by chromatography on Sephadex G-150 gave values of between 60 kDa and 70 kDa [23,24], suggesting that the AFAR isoenzymes each comprise two subunits. The recent crystallization of AKR7A1 has provided proof that rAFAR1 can indeed form a homodimer [30]. Furthermore, the crystal structure [30] has also identified that residues within the H5 and H6 secondary structures of rAFAR1 (see Figure 2) are involved in subunit dimerization. The fact that these regions are highly conserved in rAFAR2 supports the hypothesis (based on gel-filtration chromatography) that this subunit can also form a homodimer. Although it is highly probable that mouse AFAR and the human AKR7A2 and AKR7A3 enzymes are dimeric, this remains to be proven.

Catalytic specificity of rat AFAR proteins

The three AKR7 isoenzymes in rat liver resolved by anion-exchange chromatography represent the dimers rAFAR1-1, rAFAR1-2 and rAFAR2-2. The two homodimers can be readily distinguished by their specific activity towards aliphatic and aromatic aldehydes such as SSA, CBA, 4-NBA and benzaldehyde. They can also be distinguished using phenobarbital, valproate or quercitin as inhibitors of their SSA reductase activity.

From the crystal structure of AKR7A1 [30], it is predicted that the substrate-binding site of the rAFAR2 subunit is more hydrophilic than that of rAFAR1 (Table 1). This is consistent with the observations that rAFAR2-2 has a higher specific activity towards SSA and a lower specific activity towards 4-NBA than does rAFAR1-1 (Table 2). It is also consistent with the k_{cat}/K_m values calculated for rAFAR1-1, rAFAR1-2 and rAFAR2-2 for SSA and CBA (Table 3).

The AKR7 enzymes can all utilize either NADH or NADPH as cofactor in the reduction of aldehydes. A surprising feature of the specific-activity data shown in Table 2 is that both rAFAR1-1 and rAFAR2-2 appear to show a preference for either cofactor in a substrate-dependent fashion. Under standard assay conditions, with SSA or 4-NBA as substrate, rAFAR1-1 exhibits a substantially greater specific activity when NADPH is employed as cofactor than when NADH is utilized as cofactor. Conversely, rAFAR1-1 has a 3-fold higher activity towards CBA with NADH as cofactor than with NADPH. In the case of rAFAR2-2, it is substantially more active towards 4-NBA with NADPH as cofactor than with NADH. However, this enzyme exhibits a 1.8-fold greater specific activity towards SSA with NADH than with NADPH. Further experiments are required to determine whether rAFAR1-1 demonstrates greater catalytic efficiency (k_{cat}/K_m) towards CBA with NADH as cofactor than with NADPH. Similarly, further experiments are required to determine whether rAFAR2-2 demonstrates greater catalytic efficiency towards SSA with NADH as cofactor than with NADPH. At present, k_{cat} and K_m values have only been determined for the AFAR isoenzymes with NADPH as cofactor (Table 3).

Rat AFAR isoenzymes function *in vivo* as GHB synthases

The endogenous four-carbon fatty acid derivative GHB has important pharmacological functions. In the brain, it can interact with both a specific GHB receptor and the class B γ-aminobutyrate ($GABA_B$) receptor [38–40]. When given at a low dose, GHB has sedative effects, induces sleep, and stimulates secretion of growth hormone [41]. It can protect neurons against ischaemia [42], and it is also of benefit in treating alcohol addiction [43]. Administration of high doses of GHB, or accumulation of the compound as a consequence of SSA dehydrogenase deficiency, can cause petit-mal epilepsia or lethal seizures, loss of righting reflex and hypnosis [44,45]. At a biochemical level, GHB is an endogenous inhibitor of energy metabolism [46], since it can stimulate the pentose phosphate shunt pathway and diminish glucose utilization.

The 'low-K_m' SSA reductases that have been proposed to be responsible for the biosynthesis of GHB are either monomeric or dimeric enzymes with K_m values for the aldehyde of between 15 μM and 30 μM [38]. The low-K_m SSA reductase(s) in rat brain has been reported to be a monomeric protein, called SSR-2, with a K_m for the aldehyde of 28 μM [37]. An AKR with a K_m for SSA of 20 μM has been cloned from rat hippocampus that is thought to represent SSR-2 [47]. Since rAFAR1-2 and rAFAR2-2 have K_m values for SSA of about 7 μM, they can both be included amongst the low-K_m SSA reductases. Western blotting has revealed that the rAFAR2 subunit, and not rAFAR1, is expressed in the cerebral cortex, hippocampus, striatum and cerebellum of rat brain [24,48], suggesting that rAFAR2-2 contributes to GHB synthesis in the brain of the rat. The rAFAR2 subunit has been detected in neurons of rat hippocampus and striatum as well as glial cells [48]. Thus, the relative importance of rAFAR2-2 and SSR-2 in GHB production in neural tissue requires further study.

GHB is found in many organs besides the brain. For example, the levels of GHB in rat heart, kidney, liver, lung and muscle have been reported to be approx. 12 μM, 28 μM, 1.5 μM, 1.5 μM and 10 μM, respectively [49]. Immunoblotting has shown rAFAR2 is expressed in kidney, liver and lung [24], and therefore rAFAR2-2 is likely to contribute to production of GHB in these tissues. Although rat kidney and liver contain rAFAR1-1, our data in Table 3 indicate it is a 'high-K_m' SSA reductase, as it has a K_m for the aldehyde of 160 μM. It therefore

seems more likely that rAFAR1-1 acts *in vivo* as a detoxication enzyme rather than as a GHB synthase.

The rat appears to possess both monomeric and dimeric low-K_m SSA reductases. It is apparent from our study that multiple GHB synthases can occur within individual species, and that there exists a degree of heterogeneity that has not been appreciated hitherto.

Association of rAFAR2 with the Golgi apparatus

Structural similarities between AFAR isoenzymes and AKR6 proteins, along with the fact that AFAR contributes to GHB synthesis, led us to consider whether they are necessarily only present in the cytoplasm. Both subcellular fractionation and immunocytochemistry have been used to show that AFAR isoenzymes can associate with the Golgi apparatus. Enzyme assay of subcellular fractions from rat liver showed that SSA reductase activity is recovered with the Golgi apparatus, and Western blotting revealed that this fraction contained both rAFAR1 and rAFAR2 subunits. Immunocytochemistry provided further evidence that rAFAR2-2 co-localizes with Golgi markers, whereas rAFAR1-1 is primarily cytoplasmic. Together, these analyses suggest that both rAFAR1-2 and rAFAR2-2 are able to associate with the Golgi fraction.

The region of rAFAR2 that is responsible for its association with the Golgi apparatus is not known. However, it is reasonable to propose that the structural feature of rAFAR2 that directs it to the Golgi is not conserved in rAFAR1. Assuming the variant AKR core of rAFAR2 adopts the same $(\alpha/\beta)_8$ barrel structure as rAFAR1 [30], then it seems unlikely that the site of interaction will involve a β-sheet region because such regions are not particularly exposed. Therefore, the targeting of rAFAR2 to the Golgi will probably involve either the N-terminal domain, an α-helical region, loop B or loop C. Since rAFAR1 lacks the N-terminal domain, it is possible that this region is responsible for targeting rAFAR2 to the Golgi. However, a problem with this proposal comes from the fact that the N-terminal domain of rat Kvβ2 (AKR6B2) is not responsible for its docking on to pore-forming α-subunits [9,11]; this occurs through an interaction between α-helix 5 of Kvβ2 and the T1 domain of the α-subunit. Additional studies are required to determine whether the N-terminal domain of rAFAR2 is responsible for its recruitment to the Golgi apparatus, or whether it might regulate membrane channels.

Contribution of AKR7 to GHB synthesis in humans

In a species such as human that contains dimeric GHB synthases [50] it is probable that members of the AKR7 family account for the SSA reductase activity. It can be assumed that the AFAR enzymes contribute to GHB synthesis in human brain, because AKR7A2 was purified from this organ by Wermuth and his colleagues [28]. Immunohistochemistry has revealed that in human brain AKR7A2 (and possibly AKR7A3) is localized to glial cells, astrocytes, microglia and neuromelanin-containing neurons [48]. The immunoreactive AKR7 protein(s) appears to be elevated in sections of cerebral cortex and hippocampus from individuals with Alzheimer's disease [48]. Further work is required to determine the relative amounts of AKR7A2 and AKR7A3 in human brain.

Conclusions

During this study rAFAR2 has been characterized and found to possess a number of novel features. Most significantly, it contains an additional N-terminal domain that is absent from all AKR1 proteins. Unlike most members of the AKR superfamily, rAFAR2 appears to form dimers both with itself and rAFAR1. The rAFAR1-2 and rAFAR2-2 dimers have low K_m values for SSA, suggesting that they can act as GHB synthases. Consistent with this hypothesis, the rAFAR2 subunit has been found to be associated with the Golgi apparatus, an organelle that is involved in secretion of bioactive substances.

Part of this work was funded by the Mrs Elizabeth Keith Liver Cancer Fund, and we thank Mr William Keith for his interest is this work. P.J.S. was supported by the Biotechnology and Biological Sciences Research Council (94/D08200). Dr Andrew D. Cronshaw is thanked for undertaking the amino acid sequencing of rAFAR2. We are greatly indebted to Dr Andrea Gallina, Dr John M. Lucocq and Dr Matthew J. Picklo Sr. for numerous discussions and extremely helpful advice.

REFERENCES

1 Jez, J. M. and Penning, T. M. (2001) The aldo-keto reductase (AKR) superfamily: an update. Chem.-Biol. Interact. **130–132**, 499–525
2 O'Connor, T., Ireland, L. S., Harrison, D. J. and Hayes, J. D. (1999) Major differences exist in the function and tissue-specific expression of human aflatoxin B_1 aldehyde reductase and the principal human aldo-keto reductase AKR1 family members. Biochem. J. **343**, 487–504
3 Penning, T. M., Burczynski, M. E., Hung, C.-F., McCoull, K. D., Palackal, N. T. and Tsuruda, L. S. (1999) Dihydrodiol dehydrogenases and polycyclic aromatic hydrocarbon activation: generation of reactive and redox active *o*-quinones. Chem. Res. Toxicol. **12**, 1–18
4 Tipton, K. F. and Benedetti, M. S. (2002) Amine oxidases and the metabolism of xenobiotics. In Enzyme Systems that Metabolise Drugs and other Xenobiotics (Ioamides, C., ed.), pp. 95–146, Wiley, Chichester
5 Rondeau, J.-M., Tête-Favier, F., Podjarny, A., Reymann, J.-M., Barth, P., Biellman, J.-F. and Moras, D. (1992) Novel NADPH-binding domain revealed by the crystal structure of aldose reductase. Nature (London) **355**, 469–472
6 Wilson, D. K., Bohren, K. M., Gabbay, K. H. and Quiocho, F. A. (1992) An unlikely sugar substrate site in the 1.65 Å structure of the human aldose reductase holoenzyme implicated in diabetic complications. Science **257**, 81–84
7 el-Kabbani, O., Judge, K., Ginell, S. L., Myles, D. A. A., DeLucas, L. J. and Flynn, T. G. (1995) Structure of porcine aldehyde reductase holoenzyme. Nat. Struct. Biol. **2**, 687–692
8 Hoog, S. S., Pawlowski, J. E., Alzari, P. M., Penning, T. M. and Lewis, M. (1994) Three-dimensional structure of rat liver 3α-hydroxysteroid/dihydrodiol dehydrogenase: a member of the aldo-keto reductase superfamily. Proc. Natl. Acad. Sci. U.S.A. **91**, 2517–2521
9 Wilson, D. K., Nakano, T., Petrash, J. M. and Quiocho, F. A. (1995) 1.7 Å structure of FR-1, a fibroblast growth factor-induced member of the aldo-keto reductase family, complexed with coenzyme and inhibitor. Biochemistry **34**, 14323–14330
10 Ye, Q. L., Hyndman, D., Li, X. H., Flynn, T. G. and Jia, Z. C. (2000) Crystal structure of CHO reductase, a member of the aldo-keto reductase superfamily. Proteins **38**, 41–48
11 Jin, Y., Stayrook, S. E., Albert, R. H., Palackal, N. T., Penning, T. M. and Lewis, M. (2001) Crystal structure of human type III 3α-hydroxysteroid dehydrogenase/bile acid binding protein complexed with $NADP^+$ and ursodeoxycholate. Biochemistry **40**, 10161–10168
12 Khurana, S., Powers, D. B., Anderson, S. and Blaber, M. (1998) Crystal structure of 2,5-diketo-D-gluconic acid reductase A complexed with NADPH at 2.1-Å resolution. Proc. Natl. Acad. Sci. U.S.A. **95**, 6768–6773
13 Hur, E. and Wilson, D. K. (2001) The crystal structure of the GCY1 protein from S-cerevisiae suggests a divergent aldo-keto reductase catalytic mechanism. Chem.-Biol. Interact. **130**, 527–536
14 Gulbis, J. M., Zhou, M., Mann, S. and MacKinnon, R. (2000) Structure of the cytoplasmic β subunit-T1 assembly of voltage-dependent K^+ channels. Science **289**, 123–127
15 Bähring, R., Milligan, C. J., Vardanyan, V., Engeland, B., Young, B. A., Dannenberg, J., Waldschütz, R., Edwards, J. P., Wray, D. and Pongs, O. (2001) Coupling of voltage-dependent potassium channel inactivation and oxidoreductase active site of Kvβ subunits. J. Biol. Chem. **276**, 22923–22929
16 Gulbis, J. M., Mann, S. and MacKinnon, R. (1999) Structure of a voltage-dependent K^+ channel β subunit. Cell **97**, 943–952
17 Rettig, J., Heinemann, S. H., Wunder, F., Lorra, C., Parcej, D. N., Dolly, J. O. and Pongs, O. (1994) Inactivation properties of voltage-gated K^+ channels altered by presence of β-subunit. Nature (London) **369**, 289–294

18 Hayes, J. D., Judah, D. J. and Neal, G. E. (1993) Resistance to aflatoxin B_1 is associated with the expression of a novel aldo-keto reductase which has catalytic activity towards a cytotoxic aldehyde-containing metabolite of the toxin. Cancer Res. **53**, 3887–3894

19 Ellis, E. M., Judah, D. J., Neal, G. E. and Hayes, J. D. (1993) An ethoxyquin-inducible aldehyde reductase from rat liver that metabolizes aflatoxin B_1 defines a subfamily of aldo-keto reductases. Proc. Natl. Acad. Sci. U.S.A. **90**, 10350–10354

20 Ellis, E. M., Judah, D. J., Neal, G. E., O'Connor, T. and Hayes, J. D. (1996) Regulation of carbonyl-reducing enzymes in rat liver by chemoprotectors. Cancer Res. **56**, 2758–2766

21 Primiano, T., Gastel, J. A., Kensler, T. W. and Sutter, T. R. (1996) Isolation of cDNAs representing dithiolethione-responsive genes. Carcinogenesis **17**, 2297–2303

22 Kelly, V. P., Ellis, E. M., Manson, M. M., Chanas, S. A., Moffat, G. J., McLeod, R., Judah, D. J., Neal, G. E. and Hayes, J. D. (2000) Chemoprevention of aflatoxin B_1 hepatocarcinogenesis by coumarin, a natural benzopyrone that is a potent inducer of AFB_1-aldehyde reductase, the glutathione S-transferase A5 and P1 subunits, and NAD(P)H:quinone oxidoreductase in rat liver. Cancer Res. **60**, 957–969

23 Kelly, V. P. (1999) Structure and regulation of novel rat members of the aldo-keto reductase superfamily, Ph.D. Thesis, University of Dundee

24 Kelly, V. P., Ireland, L. S., Ellis, E. M. and Hayes, J. D. (2000) Purification from rat liver of a novel constitutively expressed member of the aldo-keto reductase 7 family that is widely distributed in extrahepatic tissues. Biochem. J. **348**, 389–400

25 Nishi, N., Shoji, H., Miyanaka, H. and Nakamura, T. (2000) Androgen-regulated expression of a novel member of the aldo-keto reductase superfamily in regrowing rat prostate. Endocrinology **141**, 3194–3199

26 Guengerich, F. P., Cai, H., McMahon, M., Hayes, J. D., Sutter, T. R., Groopman, J. D., Deng, Z. and Harris, T. M. (2001) Reduction of aflatoxin B_1 dialdehyde by rat and human aldo-keto reductases. Chem. Res. Toxicol. **14**, 727–737

27 Ireland, L. S., Harrison, D. J., Neal, G. E. and Hayes, J. D. (1998) Molecular cloning, expression and catalytic activity of a human AKR7 member of the aldo-keto reductase superfamily: evidence that the major 2-carboxybenzaldehyde reductase from human liver is a homologue of rat aflatoxin B_1 aldehyde reductase. Biochem. J. **332**, 21–34

28 Schaller, M., Schaffhauser, M., Sans, N. and Wermuth, B. (1999) Cloning and expression of succinic semialdehyde reductase from human brain. Identity with aflatoxin B_1 aldehyde reductase. Eur. J. Biochem. **265**, 1056–1060

29 Knight, L. P., Primiano, T., Groopman, J. D., Kensler, T. W. and Sutter, J. R. (1999) cDNA cloning, expression and activity of a second human aflatoxin B_1-metabolizing member of the aldo-keto reductase superfamily, AKR7A3. Carcinogenesis **20**, 1215–1223

30 Kozma, E., Brown, E., Ellis, E. M. and Lapthorn, A. J. (2002) The crystal structure of rat liver AKR7A1: a dimeric member of the aldo-keto reductase superfamily. J. Biol. Chem. **277**, 16285–16293

31 Ellis, E. M. and Hayes, J. D. (1995) Substrate specificity of an aflatoxin-metabolising aldehyde reductase. Biochem. J. **312**, 535–541

32 Müller, G. F., Döhr, O., El-Bahay, C., Kahl, R. and Abel, J. (2000) Effect of transforming growth factor-β_1 on cytochrome P450 expression: inhibition of CYP1 mRNA and protein expression in primary rat hepatocytes. Arch. Toxicol. **74**, 145–152

33 Leelavathi, D. E., Estes, L. W., Feingold, D. S. and Lombardi, B. (1970) Isolation of a golgi rich fraction from rat liver. Biochem. Biophys. Acta **211**, 124–138

34 Celis, J. E. (1998) Cell Biology, 2nd edn, pp. 46–55, Academic Press, San Diego

35 Praml, C., Savelyeva, L., Perri, P. and Schwab, M. (1998) Cloning of the human *aflatoxin B_1-aldehyde reductase* gene at 1p35–1p36.1 in a region frequently altered in human tumor cells. Cancer Res. **58**, 5014–5018

36 Tabakoff, B. and von Wartburg, J. P. (1975) Separation of aldehyde reductases and alcohol dehydrogenase from brain by affinity chromatography: metabolism of succinic semialdehyde and ethanol. Biochem. Biophys. Res. Commun. **63**, 957–966

37 Rumigny, J. F., Maitre, M., Cash, C. and Mandel, P. (1980) Specific and non-specific succinic semialdehyde reductases from rat brain: isolation and properties. FEBS Lett. **117**, 111–116

38 Maitre, M. (1997) The γ-hydroxybutyrate signalling system in brain: organization and functional implications. Progr. Neurobiol. **51**, 337–361

39 Bernasconi, R., Mathivet, P., Bischoff, S. and Marescaux, C. (1999) Gamma-hydroxybutyric acid: an endogenous neuromodulator with abuse potential? Trends Pharmacol. Sci. **20**, 135–141

40 Carai, M. A. M., Colombo, G., Brunetti, G., Melis, S., Serra, S., Vacca, G., Mastinu, S., Pistuddi, A. M., Solinas, C., Cignarella, G. et al. (2001) Role of $GABA_B$ receptors in the sedative/hypnotic effect of γ-hydroxybutyric acid. Eur. J. Pharmacol. **428**, 315–321

41 Van Cauter, E., Plat, L., Scharf, M. B., Leproult, R., Cespedes, S., L'Hermite-Balériaux, M. and Copinschi, G. (1997) Simultaneous stimulation of slow-wave sleep and growth hormone secretion by gamma-hydroxybutyrate in normal young men. J. Clin. Invest. **100**, 745–753

42 Vergoni, A. V., Ottani, A., Botticelli, A. R., Zaffe, D., Guano, L., Loche, A., Genedani, S., Gessa, G. L. and Bertolini, A. (2000) Neuroprotective effect of γ-hydroxybutyrate in transient global cerebral ischemia in the rat. Eur. J. Pharmacol. **397**, 75–84

43 Gallimberti, L., Ferri, M., Ferrara, S. D., Fadda, F. and Gessa, G. L. (1992) Gamma-hydroxybutyric acid in the treatment of alcohol dependence: a double-blind study. Alcohol. Clin. Exp. Res. **16**, 673–676

44 Brankack, J., Lahtinen, H., Koivisto, E. and Riekkinen, P. J. (1993) Epileptogenic spikes and seizures but not high-voltage spindles are induced by local frontal cortical application of gamma-hydroxybutyrate. Epilepsy Res. **15**, 91–99

45 Hogema, B. M., Gupta, M., Senephansiri, H., Burlingame, T. G., Taylor, M., Jakobs, C., Schutgens, R. B. H., Froestl, W., Snead, O. C., Diaz-Arrastia, R. et al. (2001) Pharmacologic rescue of lethal seizures in mice deficient in succinate semialdehyde dehydrogenase. Nat. Genet. **29**, 212–216

46 Mamelak, M. (1989) Gammahydroxybutyrate: an endogenous regulator of energy metabolism. Neurosci. Biobehav. Rev. **13**, 187–198

47 Andriamampandry, C., Siffert, J.-C., Schmitt, M., Garnier, J.-M., Staub, A., Muller, C., Gobaille, S., Mark, J. and Maitre, M. (1998) Cloning of a rat brain succinic semialdehyde reductase involved in the synthesis of the neuromodulator γ-hydroxybutyrate. Biochem. J. **334**, 43–50

48 Picklo, Sr, M. J., Olson, S. J., Hayes, J. D., Markesbery, W. R. and Montine, T. J. (2001) Elevation of AKR7A2 (succinic semialdehyde reductase) in neurodegenerative disease. Brain Res. **916**, 229–238

49 Nelson, T., Kaufman, E., Kline, J. and Sokoloff, L. (1981) The extraneural distribution of γ-hydroxybutyrate. J. Neurochem. **37**, 1345–1348

50 Hoffman, P. L., Wermuth, B. and von Wartburg, J.-P. (1980) Human brain aldehyde reductases: relationship to succinic semialdehyde reductase and aldose reductase. J. Neurochem. **35**, 354–366

Received 28 February 2002/17 June 2002; accepted 19 June 2002
Published as BJ Immediate Publication 19 June 2002, DOI 10.1042/BJ20020342